



Final Report

Role of calmodulin-regulated spectrin-associated proteins (CAMSAPs), microtubule minus end-binding proteins, on epithelial-to-mesenchymal transition in lung cancer metastasis

By Assistant Professor Varisa Pongrakhananon, Ph.D.

Final Report

Role of calmodulin-regulated spectrin-associated proteins (CAMSAPs), microtubule minus end-binding proteins, on epithelial-to-mesenchymal transition in lung cancer metastasis

Assistant Professor Varisa Pongrakhananon, Ph.D.

Department of Pharmacology and Physiology,

Faculty of Pharmaceutical Sciences,

Chulalongkorn University

Abstract

Project Code: MG5980021

Project Title: Role of calmodulin-regulated spectrin-associated proteins (CAMSAPs),

microtubule minus end-binding proteins, on epithelial-to- mesenchymal transition in lung

Lung cancer is one of the leading causes of cancer-related death worldwide

because of cancer metastasis. Cancer metastasis is a complicated multistep process

cancer metastasis

Investigator: Assistant Professor Varisa Pongrakhananon, Ph.D.

E-mail Address: Varisa.p@pharm.chula.ac.th

Project Period: May 1st, 2016 - March 31st, 2018

Abstract:

beginning with cancer cells detachment from the extracellular matrix (ECM), migration, invasion and extravasation to the circulating system. Accumulating evidences have indicated the roles of epithelial to mesenchymal transition (EMT) in cancer aggressiveness and metastasis which they are relevant with the cause of high mortality rate of cancer. The remarkable morphological changes from cobble stone-like epithelial morphology to elongated-like mesenchymal type during EMT are involved with the alteration of cytoskeleton and adhesion molecule facilitating cell motility and hence metastasis. Recent researches have emphasized on the effect of microtubule dynamic on this phenotype changes which proposed to be regulated by microtubule-binding protein. Calmodulin-regulated spectrin-associated proteins (CAMSAPs), microtubule minus-end binding family proteins, have been reported to play pivotal regulator on microtubule

behavior and proper organelle assembly during embryonic development. However, the

roles of CAMSAPs on EMT in cancer are not characterized before. This study discovered

that CAMSAP3 negatively regulated EMT process, which the CAMSAP3 knockout using

CRISPR-Cas9 system potentiated the mesenchymal-like phenotype with an upregulation of

mesenchymal markers. Furthermore, following CAMSAP3 depletion, tubulin became more

1

stabilized that required for sustain active status of protein kinase B (PKB/Akt), an EMT-regulatory protein. This study provides better understating in cancer biology on the novel function of CAMSAP3 and possible drug target against cancer metastasis.

Keywords Calmodulin-regulated spectrin-associated proteins, microtubule, epithelial to mesenchymal transition, lung cancer

Introduction to the research

Lung cancer is one of the most common causes of cancer-related death worldwide (Torre et al., 2015). Because of its aggressiveness with high metastasis rate, the 5-year survival rate is only 17% (Siegel, Miller and Jemal, 2015). Metastasis thus remains to be a major obstacle for lung cancer therapy. To establish metastasis, cancer cells need to invade nearby tissues, detach from the primary site, disseminate to the vascular system, attach and invade the basement membrane of secondary organs (Heerboth et al., 2015). Epithelial-to-mesenchymal transition (EMT) has been reported to be a crucial mechanism to achieve metastasis, which is related to the reorganization of cytoskeleton and adhesion molecule causing a dramatic transition to a mesenchymal state (Palmer et al., 2011). Over the past decade, accumulative studies indicated that metastasis cancer cells extensively exhibit mesenchymal characteristic and such behavior strongly relevant to clinical outcome (Spaderna et al., 2006; Aktas et al., 2009; Iwatsuki et al., 2010).

Although the role of actin on EMT is well characterized, the possible function of microtubule is recently begun elucidated. Microtubules, a component of cytoskeleton, have been recognized to govern the intracellular trafficking, molecular signaling and directional cell movement through their dynamic properties (Pasquier and Kavallaris, 2008). Microtubules are composed of alpha- and beta-tubulin dimers to form protofilaments displaying two ends, minus- and plus-ends. Microtubule minus-ends bind to microtubule-organizing centers (MTOCs) including centrosome and golgi complex; whereas microtubule plus-end is served as tubulin assembly or dissociated sites causing dynamic instability (Etienne-Manneville, 2013; Jiang et al., 2014). These characteristics are involved with the transition between microtubule growth or polymerization stage and shrinkage or depolarization stage allowing the interaction of microtubules to other cytoskeleton and cytoplasmic contents (Perdiz et al., 2011). Microtubule instability has been indicated to link with cellular behavior and morphology both in tissue development

and pathological diseases. For instance, the cooperation with cytoskeleton elements and several signaling molecules contributes to activate downstream effectors-related cell motility (Jiang and Akhmanova, 2011).

Several microtubule binding-proteins have been shown to regulate microtubule behaviors. Recent research gained new insights into the novel function of calmodulin-regulated spectrin-associated proteins (CAMSAPs), microtubule minus endbinding proteins. CAMSAP family consists of CAMSAP1, CAMSAP2 (CAMSAP1L1) and CAMSAP3 (Nezha), which exhibit different functions. CAMSAP1 serves as a microtubule minus-end tracking protein, whereas CAMSAP2 and CAMSAP3 share similar functions including microtubule nucleation and stabilization (Tanaka et al., 2012; Jiang et al., 2014). It has been shown that CAMSAP2 and 3 cooperate and stabilize the microtubule minusend, and promote non-centrosomal microtubule growth in human colorectal adenocarcinoma Caco-2 cells (Tanaka et al., 2012). Depletion of these proteins dramatically suppresses microtubule elongation. Similarly, Patonin, a CAMSAP3 homologue in Drosophila, was found to bind microtubule minus end and stabilized microtubules by preventing their minus end from kinesin-13-mediated microtubule depolymerization (Hendershott and Vale, 2014). Recently, it has been demonstrated that CAMSAP2 is required for maintain proper microtubule organization and cell polarization. In the absence of CAMSAP2, RFE and U2SO cells fail to establish cell polarity (Jiang et al., 2014). These studies have revealed the important role of CAMSAPs in microtubule behaviors; however, evidence is lacking for the potential involvement of CAMSAPs in EMT and cancer metastasis.

This research aims at investigating the possible impact of CAMSAPs in mesenchymal transition in lung cancer by using gene-silencing manipulation to suppress CAMSAP expressions and observation of the consequence events. Furthermore, the possible molecular signaling under these regulations will be explored using gene microarray and biochemical assays. The study is expected to provide a novel target for further drug development to inhibit cancer metastasis.

Literature review

Cancer metastasis and epidermal-to-mesenchymal transition (EMT)

Metastasis is defined as the spread of the disease from initiate site to other parts of the body, and particularly presented in several advance stage cancers which resulted in poor prognosis of the diseases. Cancer metastasis is multistep processes involving with the complex interactions of disseminating cancer cells and changing microenvironment (Hanahan and Weinberg, 2011). When the transformed cells are initiated and continued to grow at primary site, angiogenic factors are then synthesized for vascularization which increases the chance of tumor cells to circulate in blood stream or lymphatic system and colonize at distant sites. Once at new location, the extravasations of cancer cells allow the proliferation and formation of a new malignant tumor or secondary tumors which complete the metastatic processes.

In the past decade, several studies have reported that epithelial-to-mesenchymal transition (EMT) significantly plays a crucial mechanism facilitating cancer metastasis and notably relevant with clinical outcome (Iwatsuki *et al.*, 2010). EMT feature can be characterized by the morphological changes of epithelial cells to elongated fibroblast-like shape with lower cell-cell interaction and strong establishment of adhesion complex with basement membrane (Burridge and Guilluy, 2016). The looser of cell-cell contacts involved with the reduction of intercellular cohesion, and the highly front-rear polarization than those of basolateral and the reorganization of cytoskeletons favor the cell-basement membrane communication and enhance cell motility at the tumor leading edge.

Further cancer mesenchymal cells exhibits important markers including the down-regulation of E-cadherin as well as the up-regulation of N-cadherin, vimentin, Twist, SNAIL and SLUG (Mendez, Kojima and Goldman, 2010; Shih and Yang, 2011; Zhang *et al.*, 2013). E-cadherin has been recognized to be the dominant molecule found at adherent

junction that provides strong cohesive cell-cell interaction and maintains epithelial cell immobilization. The extensive downregulation of E-cadherin are observed in mesenchymal cells and significantly relevant to metastasis cancers (Iwatsuki et al., 2010). On the other hand, the aberrant upregulation of N-cadherin during EMT is found at cellcell contact instead of E-Cadherin (Wheelock et al., 2008). Similar to E-cadherin, Ncadherins require proteolytic cleavage of cytoplasmic domain, prior to activate downstream effectors, but N-cadherin mediates transduction signals that potentiate cell movement (Lade-Keller et al., 2013; Zhang et al., 2013). This cadherin switching promotes front-rear polarization affecting the intracellular trafficking, organelle localization and cytoskeleton organization (Gravdal et al., 2007; Yilmaz and Christofori, 2009). Consistency, it was reported that cadherin switching in breast tumors strongly potentiates metastasize in transgenic mice (Hulit et al., 2007). This alteration of cadherin switch is regulated by increased expressions of E-cadherin repressors including Zinc finger protein SNAI1 (SNAIL) and SNAI2 (SLUG), Smad interaction protein ZEB1 and ZEB2, helix-loop-helix transcription factor TCF3 and Twist, consequently drive EMT process (Bolós et al., 2003; Uchikado et al., 2005; Cao et al., 2015; Yang et al., 2015).

Not only high migration and invasive capacities, cancers with EMT feature also exhibit an anchorage independence behavior (Chaotham *et al.*, 2014; Unahabhokha, Chanvorachote and Pongrakhananon, 2016). Basically, majority of the epithelial cells require an adherent-dependent property for survival signaling transduction, and epithelial cells that loss of anchorage become apoptosis, termed anoikis (Guadamillas, Cerezo and Del Pozo, 2011). Anoikis is able to suppress the expansion of oncogenically transformed cells by preventing proliferation at migrating locations, which mesenchymal cancer cells acquire anoikis resistance and are able to survive and aberrantly grow in an inappropriate extracellular matrix environment. Recent studies showed that cancer cells with mesenchymal property potentiate metastasis through EGFR/PI3K/Akt pathway (Holz *et al.*, 2011; Xu, Yang and Lu, 2015). Our group also demonstrated that nitric oxide mediates mesenchymal transition in lung cancer cells which resulted in anoikis resistance

(Chanvorachote, Pongrakhananon and Chunhacha, 2014; Chanvorachote, Pongrakhananon and Chaotham, 2016). The association of EMT and anoikis resistance has been also demonstrated to be involved with loss of E-cadherin expression at cell-cell interaction and tumor growth factor β (TGF β)- and Wnt pathway-mediated cell polarity (Frisch, Schaller and Cieply, 2013).

During a past few years, EMT has gained attention in cancer field since it has been discovered to be the pivotal metastasis mechanism utilized by aggressive cancer. Several researches have been conducted to identify the key regulator driving mesenchymal properties in metastasis tumor cells. The better understanding of this phenomenon would provide potential target and development of new drug against metastasis, and improve clinical outcome.

Microtubule and microtubule minus-end binding protein CAMSAPs

The biology of microtubule cytoskeleton has been discovered to regulate cell cycle, morphogenesis and migration. Evidences in metastasis cancer, microtubules play an important role on the establishment of cell polarity that favor cell locomotion. Cell polarity has been shown to cause by microtubule asymmetry that microtubule polymerization is found densely at the leading edge than cell body and the rear edge (Kaverina and Straube, 2011). In non-migrated epithelial cells, microtubules orientate radially, in contrast to those of migrated cells, microtubule network is asymmetry, which this microtubule pattern is determined by the position of nucleus. In order to migrate, microtubule-organizing centers (MTOCs) mainly mediated this polarization by localization at the front of nucleus into the directional movement, and microtubules are then rapidly polymerized toward the front edge, whereas microtubules behind nucleus exhibit slower elongation and/or become shrinkage. During cell protrusion, microtubule polymerization generates the driving force, which support actin filament pushing cell membrane to form lamellipodia (Etienne-Manneville, 2013). Several studies report that this dynamic instability was regulated by microtubule binding proteins.

Recently, microtubule minus-end binding proteins were gained new insight on developmental biology research. Generally, microtubule minus-ends are capped with gamma-tubulin ring complex (gTURC) attached to centrosome, and microtubule elongation is occurred from plus-end to cell periphery. However, in some cell types, microtubules minus-ends are capped with minus-end binding proteins instead, which served as microtubule originated sites, and microtubule polymerization is initiated extending to cell cortex. These non-centrosomal microtubules are found especially in epithelial and neuronal cells, which this phenomenon provides the microtubule orientation differ from fibroblast and other cell types (Akhmanova and Hoogenraad, 2015) (Figure 1). In fibroblast cells, microtubules are originated from the center where centrosome locates, whereas epithelial cells contain both centrosomal and noncentrosomal microtubules, in which minus-ends are pointed out to apical surface in opposite direction to their plus-ends. In neuronal cells, non-centrosomal microtubules are predominant which the bidirectional microtubule orientation was found in dendrite, in contract to the axon, whose microtubule plus-ends outgrow to growth cone. This suggests that the different microtubule orientation provides the distinct physiological behaviors among cell types.

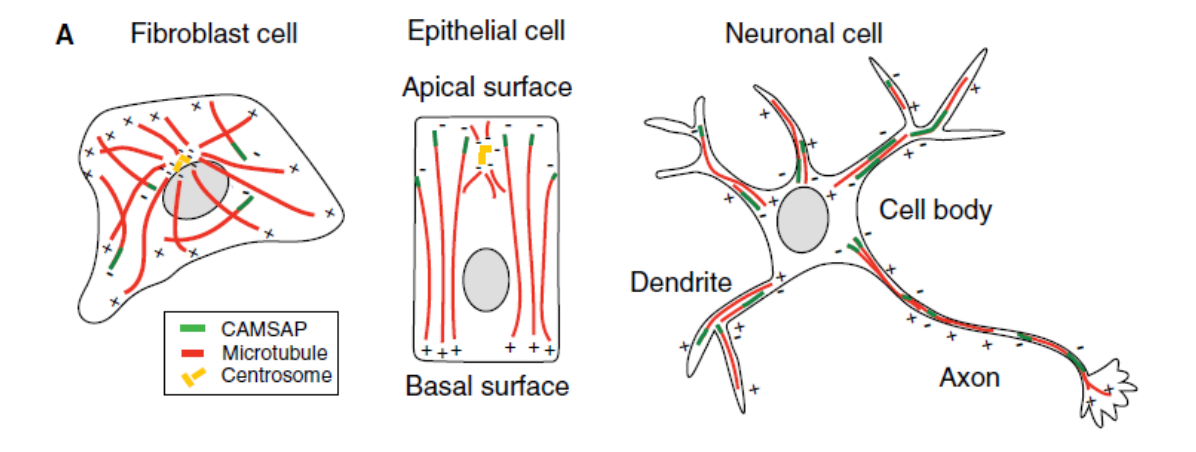


Figure 1 Microtubule organizations in different cell types (Akhmanova and Hoogenraad, 2015).

Non-centrosomal microtubules are involved with various pivotal cellular processes through their ability to depolarize involving both cellular trafficking of organelle and signaling molecules. The stabilization of microtubule minus-ends is regulated by several capping proteins including Calmodulin-regulated spectrin-associated proteins (CAMSAPs). CAMSAPs, minus-end binding protein family, are consisted of CAMSAP1, CAMSAP2 (CAMSAP1L1) and CAMSAP3 (Nezha) (Akhmanova and Hoogenraad, 2015). They are characterized by three conserved regions; carboxy-terminal CKK, amino-terminal calponin homology CH and coiled-coil (CC) domains (Figure 2).

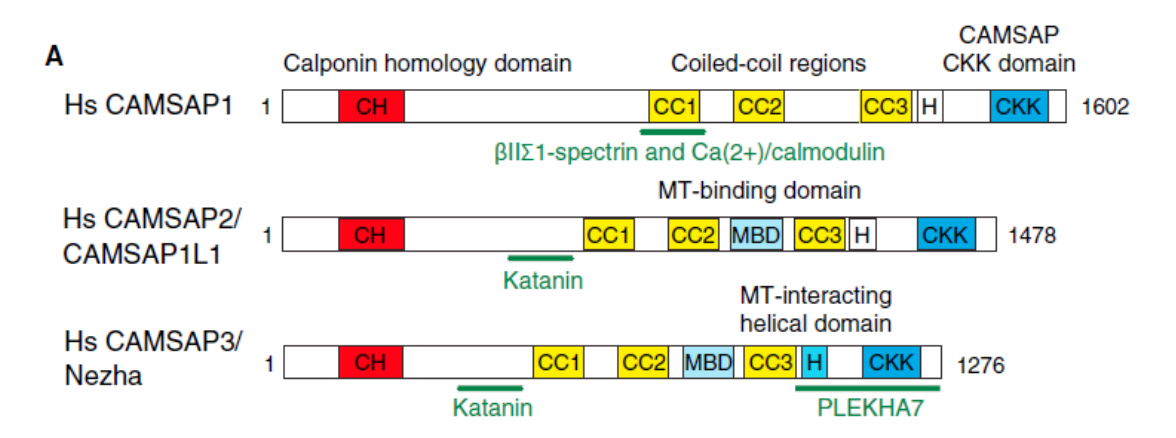


Figure 2 Structure of CAMSAPs family proteins (Akhmanova and Hoogenraad, 2015).

Although CAMSAPs share similar functional domains, some proteins sequences are difference. Time lapse imaging in HEK293T cells transfected with fluorescent-tagged CAMSAPs demonstrated that CAMSAP1 associates to microtubule minus-ends served as tracking protein, whereas CAMSAP2 and CAMSAP3 also stabilize microtubule minus end (Tanaka *et al.*, 2012; Nagae, Meng and Takeichi, 2013; Jiang *et al.*, 2014). In the absence of CAMSAP2 and CAMSAP3, non-centrosomal microtubules are significantly disappeared after nocodazole (a microtubule depolarizing drug) treatment, suggesting that both CAMSAPs play an important role on either prevention of microtubule depolarization or being microtubule nucleated sites. This data was supported by that Patronin, a CAMSAP3 homologue in *drosophila*, inhibits kinesin-13 depolymerase-mediated microtubule catastrophes (Hendershott and Vale, 2014). Nocodazole experiment also demonstrated that after microtubule depolarization, the new microtubules are able to grow from

CAMSAP2 and CAMSAP3, indicating the important of these proteins as seed for microtubule outgrowth (Tanaka *et al.*, 2012; Jiang *et al.*, 2014). Furthermore, CAMSAP2 and CAMSAP3 were showed to bind with Katanin, a microtubule severing protein, to regulate the proper length of non-centrosomal microtubule (Jiang *et al.*, 2014).

Interestingly, it has showed that nocodazole treatment impedes the cell motility in Hela cells (Ganguly *et al.*, 2012), similarly that CAMSAP2 depleted RPE cells fail to establish movement (Jiang *et al.*, 2014). However, this study did not describe underlying mechanism regarding CAMSAP2 promotes cell locomotion as well as the function of other CAMSAP proteins on cell polarity since their functions are cell-type specific. Although most research mainly emphasis on the role of CAMSAPs on microtubule behavior in developmental biology, there are no report on the association of CAMSAPs and EMT phenotype in cancer pathology. This research will define the possible role of CAMSAPs on the mesenchymal transition in human lung carcinoma cell lines originated from advanced stage cancer. Furthermore, the information obtained from this study might provide potential target for suppression of cancer metastasis.

Objectives

- 1) To investigate the role of CAMSAP2 and CAMSAP3 on epidermal-tomesenchymal transition and metastasis in cancer cells
- 2) To identify the underlying mechanism in which CAMSAPs mediate epidermalto-mesenchymal phenotypes in cancer cells

Research Methodology

1) Reagents

Taxol, nocodazole, LY294002 and DAPI were purchased from Sigma. Antibody to CAMSAP3 was kindly gifted from Professor Masatoshi Takeichi (RIKEN CDB, Japan). Other antibodies were purchased as follows: rabbit anti-CAMSAP2 (Proteintech, 17880-1-AP), rabbit anti-Slug (Cell Signaling Technology, 9585), rabbit-anti ZEB1 (Cell Signaling Technology, 3396), rabbit anti-E-cadherin (Cell Signaling Technology, 3195), rabbit anti-N-cadherin (Cell Signaling Technology, 13116), rabbit anti-phosphorylate Akt (S437, Cell Signaling Technology, 9271), rabbit anti-Akt (Cell Signaling Technology, 9272), mouse anti-GAPDH (Cell Signaling Technology, 97166), mouse anti-tubulin (Sigma, T6199), mouse anti-acetylated tubulin (Sigma, T7451), mouse anti-paxillin (BD Biosciences, 610051), mouse anti-His (MBL, D291-3) and rat- α tubulin (Millipore, MAB1864). The secondary antibodies used were: goat Alexa Fluor 488-, 568-, 555- and 647-conjugated anti-mouse, rabbit or rat IgG (1:000 for immnunofluorescence, Invitrogen), sheep HRP-conjugated anti-mouse and anti-rabbit IgG (1:5000 dilution for immunoblotting, Cell Signaling Technology).

2) Cell culture

H460, H23, A549 and HeLa cells were purchased from American Type Culture Collection. H460 and H23 cells were cultured in RPMI medium supplemented with 10% fetal bovine serum, 2 mM L-glutamine, and 100 units/mL penicillin/streptomycin. A549 and HeLa cells were cultured in DMED with similar supplements. Cells were maintained in 37°C and 5% CO₂ environment.

3) Plasmid and transfection

sgRNAs sequence were designed to target *CAMSAP3* exon-1 by an online tool (http://crispr.mit.edu/) as follows:

sgRNA#1, 5'-CACCGACTAGAAAGGTCCTCCGCAG-3'; and sgRNA#2, 5'-CACCGAGCCCAGCCCAGTCCGAGCG-3'.

The CRISPR/Cas9 plasmid was constructed as described previously with some modifications (Ran *et al.*, 2013). Plasmids expressing sgRNA were cloned by annealing each DNA oligo, and ligated into pScas9-2A-puro (Addgene) at Bsbl site. The sgRNA sequencing of vectors were conducted using U6F primer. Transfection was performed using Lipofectamine[®] 2000 (Invitrogen), according to manufacturer's instruction. Briefly, 2 µg of each plasmid in optiMEM media were mixed with 6 µl of Lipofectamine[®] 2000. After 30 min, the mixture was dropped onto cells in culture, and cells were incubated at 37°C for 6 h. The addition of antibiotic puromycin was performed next day. The expression of CAMSAP3 was confirmed by immunoblotting, immunofluorescence and real-time qPCR. The *CAMSAP3* knockout cell was designated as H460/C3ko cell, and the control mock transfectant was called H460/Ctrl cell.

For constructing a CAMSAP3-expressing plasmid, full-length *CAMSAP3* cDNA with a His-tagged sequence on its 3' end was cloned into pCANw. The EB1-expressing plasmid with C-terminally RFP-tag was kindly provided by Dr. Mimori-Kiyosue (RIKEN). Transfection was performed using Lipofectamine[®] 2000 (Invitrogen), according to the manufacturer's instruction. Briefly, 3 µg of plasmid in optiMEM media were mixed with 6 µl of Lipofectamine[®] 2000. After 30 min, the mixture was dropped onto cells in culture, and cells were incubated at 37°C for 6 h. Stable transfectants were isolated by culturing cells in a medium supplemented with antibiotic G418 (400 µg/ml) for at least 7 d, and by subsequent cloning. Expression of exogenous DNA was confirmed by immunoblotting or immunofluorescence assay.

4) siRNA transfection

Cells were transfected with siRNAs specific for target proteins by lipofectamine $^{\$}$ RNAiMAX, according to the manufacturer's protocol (Invitrogen). Stealth RNAis targeting CAMSAP2, CAMSAP3 or α -TAT1 with the following sequences and control siRNA were purchased from Invitrogen:

siCAMSAP2, 5'-UCUCGAAUCUGUUUCUGUGGAGAGG-3';

siCAMSAP3, 5'-ACAGUGGCAGCAGUUCUCCUGUCUU-3';

si α -TAT1#1, 5'-ACCGCACCAACTGGCAATTGA-3'

si α -TAT1#2, 5'-GAGCCAUUAUUGGUUUCCUCAAAGU-3'.

Briefly, 100 nM of siRNAs in optiMEM media were incubated with Lipofectamin[®] RNAiMAX mixture for 15 min at room temperature, then dropped onto cells, and cells were incubated at 37°C for another 6 h. At 72 h after transfection, cells were subjected to Western blot analysis or immunofluorescence assay.

5) Cell migration assay

For wound healing assay, 1.5×10^4 cells were seeded into each well of the 24-well culture plate. After cells had reached confluence, wound scratches were generated using a pipette tip, and detached cells were removed by washing with PBS. Images were acquired at indicated time points and wound area was quantified by Image-J software. For transwell migration assays, 5×10^4 cells in a serum-free medium were placed in the upper chamber with a 8.0 µm pore-sized membrane, and a complete culture medium was added into the lower chamber. After 24 h, cells at the upper-side of the membrane were swabbed out and those at the underneath were fixed with cold methanol at -20°C for 5 min, and incubated with DAPI for 10 min. Migrating cells were imaged randomly using a fluorescence microscope (Olympus IX51).

6) Cell proliferation assay

Two-thousand cells were seeded into each well of 96-well plates, preparing at least 5 replicates. After the indicated times, medium was replaced with the MTT solution (0.5 mg/ml) and incubated at 37 °C for 4 h. A 100 μ l of dimethyl sulfoxide (DMSO) was placed to dissolve formazan products, and the absorbance was measured at 570 nm using microplate reader. Cell proliferation was calculated as a relative value to the value at the initial time point.

7) Soft agar colony formation assay

A 24-well plate was coated with 0.3% agarose in the complete medium as the bottom layer. After solidification, 10³ cells were suspended in 0.5 % agarose in the medium and seeded onto the bottom layer. Cells were incubated for 14 d, to which the medium was added every 2 d to prevent dryness. Cells were then stained with 0.01% crystal violet in 10% ethanol for 30 min at room temperature. After washing several times with deionized water, the colonies were captured, and their number was counted and presented as a relative number to the control cells, using Image-J software with particle analysis plugin.

8) Western blot analysis

Cells were incubated in lysis buffer containing 20 mM Tris-HCl (pH 7.5), 1% Triton X-100, 150 mM sodium chloride, 10% glycerol, 1 mM sodium orthovanadate, 50 mM sodium fluoride, 100 mM phenylmethylsulfonyl fluoride and a commercial protease inhibitor cocktail (Roche Molecular Biochemicals) for 30 min on ice. The cell lysates were collected, and the protein content was determined using the Bradford method (Bio-Rad Laboratories, Hercules, CA). Equal amounts of protein from each sample (60 µg) were denatured by heating at 95°C for 5 min with Laemmli loading buffer and subsequently loaded onto a 10% SDS-polyacrylamide gel. After separation, the proteins were transferred onto 0.45-um nitrocellulose membranes (Bio-Rad). The transferred membranes were blocked for 1 h in 5% nonfat dry milk in TBST (25 mM Tris-HCl (pH 7.5), 125 mM NaCl, 0.05% tween 20) and incubated with the specific primary antibodies at 4°C overnight. The membranes were washed twice with TBST for 10 min and incubated with horseradish peroxidase-coupled isotype-specific secondary antibodies for 2 h at room temperature. The immune complexes were detected by enhancing with a chemiluminescence substrate (Supersignal West Pico; Pierce) and quantified using analyst/PC densitometry software (Bio-Rad).

9) Microtubule sedimentation assay

Cells were treated with either 10 μ M nocodazole for 1 h at 4°C, 1 μ M taxol for 5 min at 37°C or DMSO as control. The sample was lysed by a microtubule stabilizing buffer (MTB) containing 80 mM PIPES, 80 mM K-1,4-piperazinediethanesulfonic acid, pH 6.8, 1mM EGTA, 1 mM MgCl₂, 0.5% (vol/vol) Nonidet P-40, 20 mM NaF, 0.5% sodium deoxychlorate, 0.1 mM phenylmethylsulfonyl fluoride, and protease inhibitor cocktail; Roche) for 5 min at 37°C in dark. The lysate was fractionated into a pellet and supernatant by centrifugation at 17,400 xg for 15 min at 30°C. The pellet was washed by MTB without detergents, and resuspended with MTB in an equal volume of supernatant. Both pellet and supernatant fractions were boiled at 95°C with a sampling buffer, and subjected to Western blot analysis.

10) RNA extraction and quantitative real-time polymerase chain reaction

Total RNA was isolated from cells using GENEzol reagent (Geneaid). RNA (1 μ g) was reversed to cDNA using ProtoScript II Reverse transcriptase (New England BioLabs) as described by the manufacture's instruction. mRNA expression of CAMSAP3, E-cadherin, N-cadherin, Snail, Slug and ZEB1 were measured by Bio-Rad T100 Thermal Cycler (Bio-Rad) using 2x iTaq Universal SYBR Green Supermix (Bio-Rad). The primer paired used were indicated in Table 1. The thermo cycling condition was set as follows: 95°C for 10 min, 35 cycle at 95°C for 30 sec, and 60°C for 30 sec. The data were calculated as $\Delta\Delta$ Ct method (Livak and Schmittgen, 2001). Each sample was performed in triplicate.

Table 1 Sequences of the primers used in the experiments

Genes	Forward primer	Reverse primer
CAMSAP3	5'-AACGGGACTGGGAAAATGG-3'	5'-TGGGTTCTTTGTACAGCCG-3'
ECAD	5'-TTAAACTCCTGGCCTCAAGCAATC-3'	5'-TCCTATCTTGGGCAAAGCAACTG-3'
NCAD	5'-GACCGAGAATCACCAAATGTG-3'	5'-GCGTTCCTGTTCCACTCATAG-3'
SNAIL	5'-CTAGCGAGTGGTTCTTCTGC-3'	5'-GTAGTTAGGCTTCCGATTGGG-3'
SLUG	5'-AGCATTTCAACGCCTCCA-3'	5'-GGATCTCTGGTTGTGGTATGAC-3'
ZEB1	5'-AAGGGCAAGAAATCCTGGG-3'	5'-TCTGCATCTGACTCGCATTC-3'
VIMENTIN	5'-ACCCTGCAATCTTTCAGACAG-3'	5'-GATTCCACTTTGCGTTCAAGG-3'
GAPDH	5'-ACATCGCTCAGACACCATG-3'	5'-TGTAGTTGAGGTCAATGAAGGG-3'

11) Immunofluorescence assay

Cells were fixed with 4% paraformaldehyde in PBS for 20 min at room temperature in dark, and permeabilized by 0.1% Triton X in PBS for 10 min. For microtubule staining, cells were fixed with cold methanol for 5 min at -20 °C. Non-specific signals were blocked by treatment with 3% BSA for 30 min or longer, followed by incubation with the indicated primary antibodies overnight at 4°C. Cells were wash with PBS and incubated with a secondary antibody for 2 h at room temperature in dark. After washing with PBS containing DAPI, coverslips were washed with deionized water, and subsequently mounted by FluorSave (EMD). Confocal images were acquired by either Zeiss LSM880 (Carl Zeiss) through a Plan-Apochromat 63x/1.40 N.A. or Leica TCS SP8 (Leica Microsystems) with 100x oil immersion objective lens. Image preparation and analysis were performed using Image-J software.

12) Immunoprecipitation

Cells were dissolved in lysis buffer containing 60 mM K-Pipes, pH 7.0, 25 mM Hepes, 10 mM EGTA, 2 mM MgCl₂, 1% Nonidet P-40, and a commercial protease inhibitor cocktail (Roche Molecular Biochemicals). After centrifugation, supernatants were collected

and precleared with protein G-conjugated Sepharose beads (GE Healthcare) for 1 h, incubated with antibody against each CAMSAP for 12 h. After that, lysates were incubated with protein G-conjugated Sepharose beads for 1 h. Beads were then washed five times with the lysis buffer containing 0.5% Nonidet P-40. Precipitates were eluted with a sample buffer and boiled at 95°C for 10 min, separated by SDS/PAGE, and analyzed by western blotting.

13) Statistical Analysis

All experiments are performed at least 3-4 times. For quantitative experiments, mean data from independent experiments are normalized to the results from cells in the control group. A statistical analysis between two groups is verified by Student's t test, and to compare to multiple groups, an analysis of variance (ANOVA) with a post-hoc test is conducted. A P-value of less than 0.05 was considered statistically significant.

Experimental Designs

1) Investigation of CAMSAP3 localization

Cells were co-transfected with plasmid containing pCA-CAMSAP3-His and pCA-EB1-RFP using Lipofectamine[©]2000. Transfected cells were cultured onto coverslip. CAMSAP3-His, tubulin plus-end tracking protein EB1-RFP and tubulin were analyzed by immunofluorescence assay, and captured by confocal microscope.

2) Investigation the correlation of CAMSAP3 expression and cell motility

H460, H23 and Hela cells were lysed and endogenous CAMSAP3 level was determined by immunoblotting. The migration activity among these cells were evaluated by wound healing assay at 0, 24 and 48 h. To exclude the effect of cell proliferation, cell growth was analyzed by cell proliferation assay.

3) CAMSAP3 knockout cells generation

To determine whether CAMSAP3 regulates mesenchymal transition, CAMSAP3 knockout was conducted. H460 cells were transfected with either pScas9-2A-puro targeting human CAMSAP3 or scramble (Invitrogen) using Lipofectamin[©]2000 for 6 h. Cells were cultured with puromycin for selection of CAMSAP3 knockout stable clone. To confirmation of CAMSAP3 knockout efficiency, CAMSAP3 knockout and control cells were cultured onto 6-well plate, and CAMSAP3 expression was determined by western blot analysis using specific antibodies against CAMSAP3. Protein expressions were quantified by densitometry analysis comparing to control transfected cells. Furthermore, RNA was extracted from CAMSAP3 knockout and control cells and evaluated the mRNA expression by qRT-PCR using specific primer to CAMSAP3 (Table 1).

4) Investigation the effect of CAMSAP3 on EMT phenotypes

After CAMSAP3 knockout cells were established, cells were cultured onto 24well plate and migrating transwell for migration assay, 12-well plate containing agarose for soft agar assay, and 6-well plate for western blot analysis. After 36 h, cells were further evaluation for EMT characteristics.

- Cell morphology

CAMSAP3 knockout and control cells were cultured onto 96-well overnight.

Cell morphology was captured by inverted microscope.

- Cell migration

Cell migration was determined by wound healing and transwell migration assay. For wound healing assay, transfected cells were cultured onto 24-well plate. Cell monolayer was scratched to generate the wound space and captured by inverted microscope (Olympus IX51 with DP70) using 10X magnification every 0, 12, 18, 24, and 48 h. The wound spaces from at least ten fields/sample were measured at different time points by ImageJ (NIH), and the average areas of each sample were plotted relatively to time 0 and control group.

For transwell migration assay, transfected cells were cultured onto the upper chamber in serum free media. The migrated cells at the underside of membrane were evaluated comparing with control transfected cells.

- Anchorage-independent growth

Transfected cells were suspended in media containing agarose and subjected to soft agar colony formation assay. After 2 weeks, the size and number of colonies formed were visualized and scored using inverted microscope compared to control transfected cells.

- Actin stress fiber and focal adhesion formation

CAMSAP3 knockout and control cells were cultured onto coverslip overnight. Immunofluorescence assay was performed using antibody to paxillin and phalloidin. Images were captured under confocal microscope.

- EMT marker protein and mRNA expressions

CAMSAP3 knockout and control cells were cultured onto 6-well plate, and EMT marker protein expressions were determined by Western blot analysis using specific

antibodies to E-Cadherin, N-Cadherin, Slug and ZEB1. Protein expressions were quantified by densitometry analysis comparing to control transfected cells. Furthermore, RNA was extracted from CAMSAP3 knockout and control cells and evaluated the mRNA expression to EMT markers by qRT-PCR using specific primer (Table 1).

5) Confirmation the effect of CAMSAP3 on EMT phenotype in CAMSAP3 knockdown cells by small interference RNA

A549, H460 and HeLa cells were transfected with siRNA against CAMSAP3. CAMSAP3 expression and EMT protein makers were evaluated by immunoblotting. Cell motility was analyzed by wound healing assay.

6) Investigation the effect of CAMSAP3 on microtubule dynamic

CAMSAP3 knockout and control cells were cultured onto coverslip. Tubulin acetylation, tubulin detyrosination, and total tubulin were analyzed by immunofluorescence and immunoblotting assays. Furthermore, tubulin dynamic was evaluated among cell line H460, H23 and HeLa cells by immunoblotting assay.

7) Investigation the effect of CAMSAP3 on Akt activity

Akt activation (Phophorylated Akt) and total Akt were determined by immunofluorescence and immunoblotting assays in CAMSAP3 knockout and control cells. Furthermore, Akt activation was also evaluated among cell line H460, H23 and HeLa cells by immunoblotting assay.

To confirm whether CAMSAP3 deletion causes an Akt overactivation, CAMSAP3 knockout cells were treated with PI3K inhibitor, LY294002. Akt phosphorylation and total Akt level were determined by immunoblotting assay. Furthermore, the migration rate following LY294002 treatment was evaluated in CAMSAP3 knockout cells by wound healing assay.

8) Investigation the possible interaction between CAMSAP3 and Akt

H460 cells were stable transfected with pCA-CAMSAP3-His. Immunoprecipitation was performed by pulling down using anti-His antibody and immunoblotting for Akt and phosphorylated Akt. Furthermore, cells were cultured onto coverslip and double stained for His with either Akt or phosphorylated Akt. Images were captured under confocal microscope.

9) Investigation the interaction between phosphorylated Akt and tubulin

H460 cells were treated with either Taxol, nocodazole or DMSO as control for 1 h. Cells were lysed and subjected to tubulin separation by microtubule sedimentation assay. The expression of phosphorylated Akt and tubulin in soluble and precipitate fractions were analyzed by immunoblotting.

10) Investigation the effect of tubulin dynamic on the Akt activity

H460 cells were pretreated with nocodazole or DMSO as control for 5, 10 and 15 min followed by treatment with taxol for 15 min. Phosphorylated Akt was determined by immunoblotting. To test whether tubulin acetylation is required for Akt activation, firstly, the interaction of phosphorylated Akt with tubulin acetylation was evaluated in CAMSAP3 knockout and control cells by immunofluorescence assay. Second, CAMSAP3 knockout cells, with high level of tubulin acetylation, were transfected with siRNA targeting to α tubulin acetyltransferase (α TAT). Tubulin acetylation and phosphorylated Akt were then analyzed.

11) Investigation the reversal effect of CAMSAP3 overexpression in CAMSAP3 knockout cells

CAMSAP3 knockout cells were transfected with pCA-CAMSAP3-His or control plasmid. The endogenous CAMSAP3 and CAMSAP3-His were determined by immunoblotting. Cell morphology was captured under inverted microscope. Akt activation

and tubulin acetylation were determined by immunoblotting and immunofluorescence assays.

To investigate whether CAMSAP3 overexpression could suppress mesenchymal phenotypes in CAMSAP3 knockout cells, EMT protein markers and their mRNA were analyzed by Immunoblotting and qRT-PCR in CAMSAP3 knockout cells transfected with either pCA-CAMSAP3-His or control plasmid. Along with, cell migration rate was evaluated by wound healing assay.

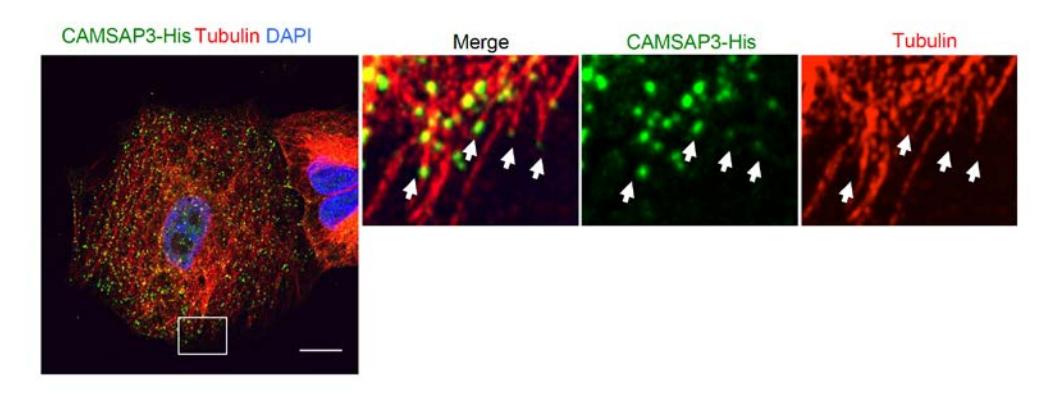
12) Investigation the effect of CAMSAP2 on EMT process

H460 cells were transfected with siRNA targeting CAMSAP2. CAMSAP2 expression was then analyzed by immunoblotting, and cell migration rate was determined by wound healing assay.

1. CAMSAP3 localized at the minus-end of tubulin.

CAMSAP3 distribution among cell types varies. For instance, it is mainly anchored to non-centrosomal microtubules at the apical surface of polarized Caco2 cells (Toya *et al.*, 2015). CAMSAP3 localization in cancer H460 cells was therefore investigated. CAMSAP3 staining exhibited punctate signals binding to tubulin ends throughout the cytoplasm (Fig. 1A) and did not overlap with staining for exogenous RFP-tagged plus-end-tracking protein 1 (EB1-RFP), a microtubule plus-end-binding protein (Fig. 1B), indicating the existence of non-centrosomal microtubules with their minus-end decorated with CAMSAP3 in these cells.

Α



В

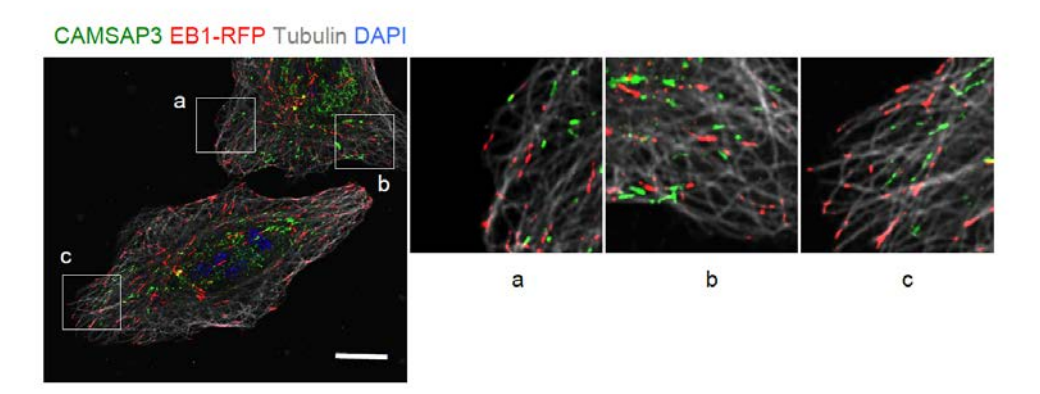


Figure 1 CAMSAP3 expression and migration profile in cancer cells. A Representative image of exogenous CAMSAP3-His (green), α -tubulin (red) and DAPI (blue) in H460 cells. B. Immunofluorescence of CAMSAP3 (green), EB1-RFP (red), α -tubulin (grey) and DAPI (blue) in HeLa cells. (Scale bar 10 μ m)

2. CAMSAP3 level was correlated with migratory activity of cancer cells.

Microtubules have a crucial role in cellular behaviors including cell motility (Kaverina and Straube, 2011). Therefore, we investigated whether CAMSAP3, a microtubule minus-end-binding protein, regulated this cell activity. The results showed that HeLa cells with the highest levels of CAMSAP3 displayed the lowest motility rate; therefore, the largest wound area remained (Fig. 2A and B). On the other hand, H23 and H460 cells with comparable lower levels of CAMSAP3 were more migratory. Cell proliferation assays were performed to exclude the possibility of cell division causing a narrow wound area, and all tested cells had a similar proliferation rate (Fig. 2C).

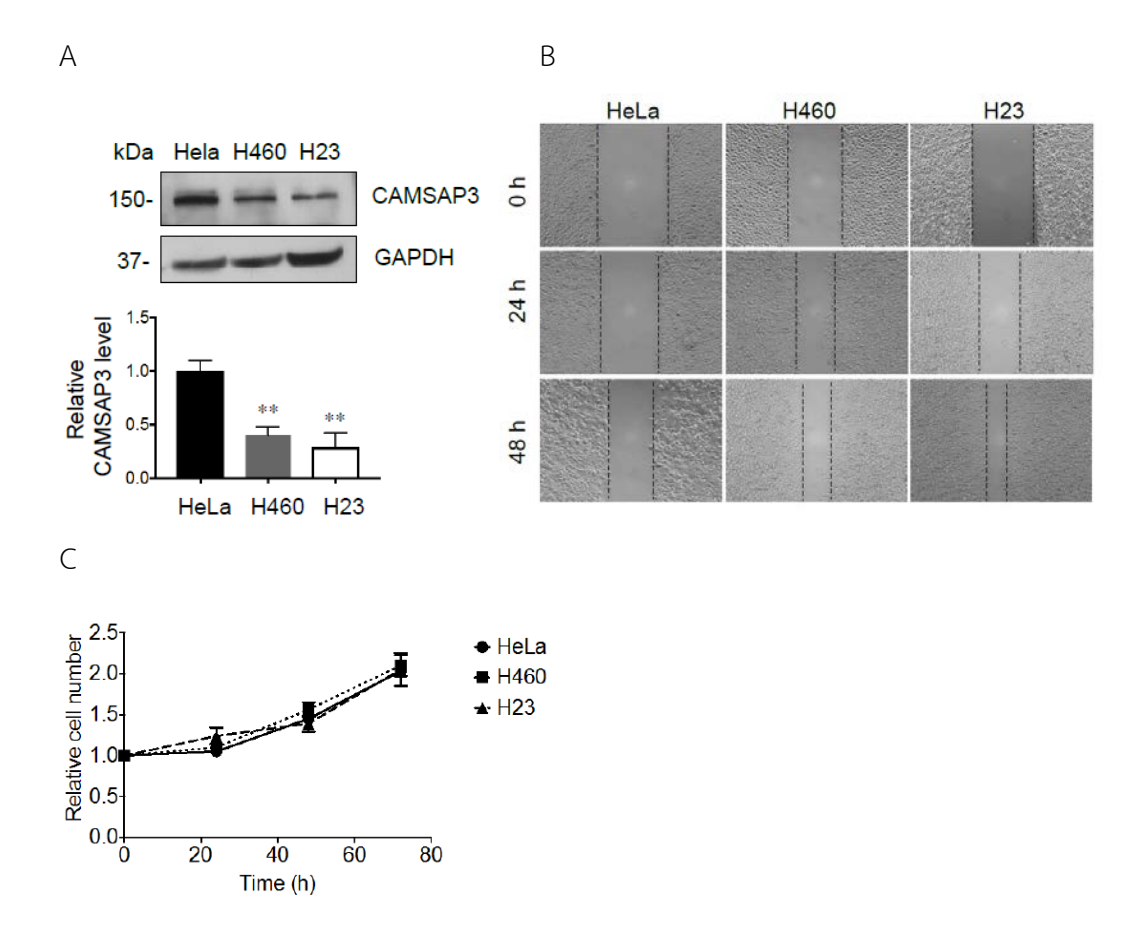


Figure 2 A. Immunoblotting revealed CAMSAP3 expression levels in HeLa, H460 and H23 cells. Each plot was mean \pm SEM from triplicate-independent experiments, compared to GAPDH, which served as a loading control. **, P < 0.01 vs HeLa cells. B. Cell migration was examined with a wound healing assay for 0-48 h. Wound area was presented as a relative

value to the initial time point. Data were mean \pm SEM from triplicate experiments. *, P < 0.05; **, P < 0.01 vs time 0 h. C. Cell proliferation of HeLa, H460 and H23 cells was analyzed at 24, 48 and 72 h. Data were mean \pm SEM from triplicate-independent experiments.

3. CAMSAP3 negatively regulates cancer cell migration through epithelial-to-mesenchymal transition

To investigate the possible role of CAMSAP3 in the regulation of EMT, we generated CAMSAP3 knockout H460 cells using the CRISPR-Cas9 system (Fig. 3A and B). Camsap3 knockout cells were termed H460/Camsap3 KO (H460/C3ko) cells, and their protein and mRNA expressions disappeared (Fig. 4A and B). Western blot analysis revealed that EMT markers, including N-cadherin (N-cad), Slug and ZEB1, were upregulated. In contrast, the epithelial marker, E-Cadherin (E-cad), which was downregualted (Fig. 4A). The changes in protein levels corresponded to the changes in mRNA levels, except in the case of slug (Fig. 4B). It is possible that the post-transcriptional regulation of slug might be influenced by the Camsap3 knockout. Interestingly, a spindle-like mesenchymal morphology, together with intense actin stress fibers and an increase in the focal adhesion protein paxillin, appeared in Camsap3-depleted cells (Figs. 5A and B), similar to what was observed in TGF- β -treated cells (Fig. 6). Wound healing and transwell migration assays demonstrated that the wound area was extensively decreased and that the number of migrating cells was significantly enhanced in the absence of CAMSAP3 (Figs. 5C and D). Although H460/Camsap3 KO cells exhibited a slightly lower growth rate, this behavior did not affect EMT activity. Since the EMT process provides a survival mechanism for cancer cells in a detached environment, colony formation assays on soft agar as in a cell detachment model were then carried out. The results showed that Camsap3-depleted cells had enriched growth, along with an increase in the number of colonies formed (Fig. 5E). To elucidate whether CAMSAP2 participates in phenotypic changes after CAMSAP3 removal, CAMSAP2 expression was investigated. Interestingly, in the absence of CAMSAP3,

CAMSAP2 remained unchanged, indicating the specific role of CAMSAP3 in this cellular tranformation (Fig. 7).

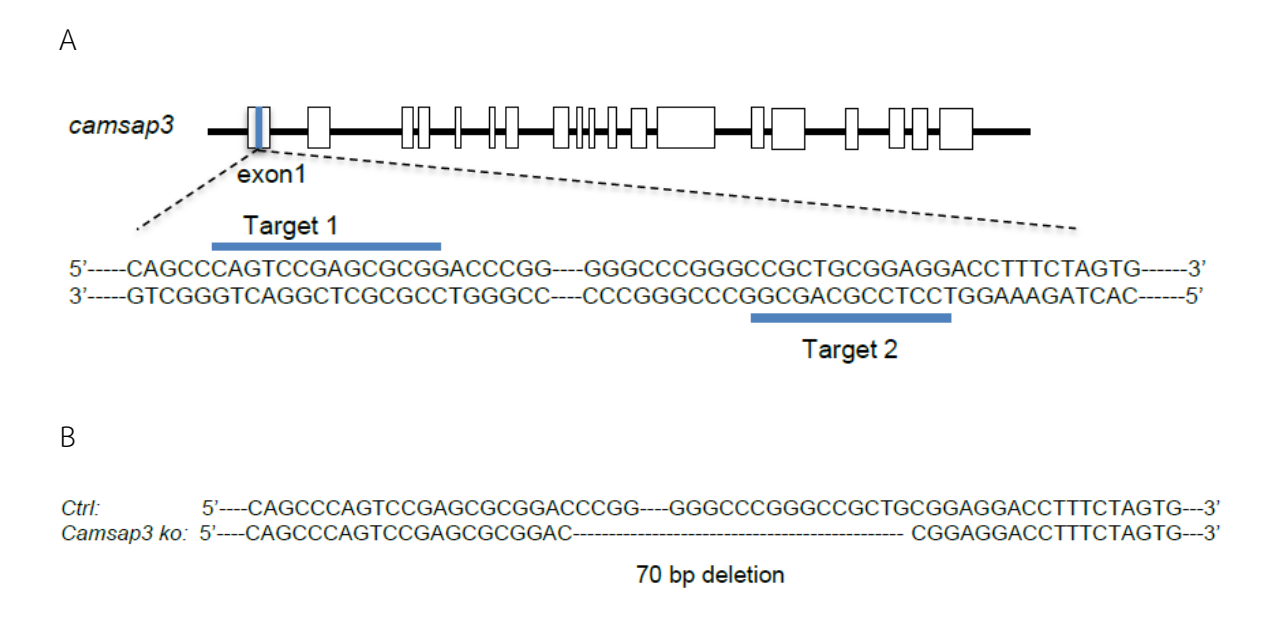
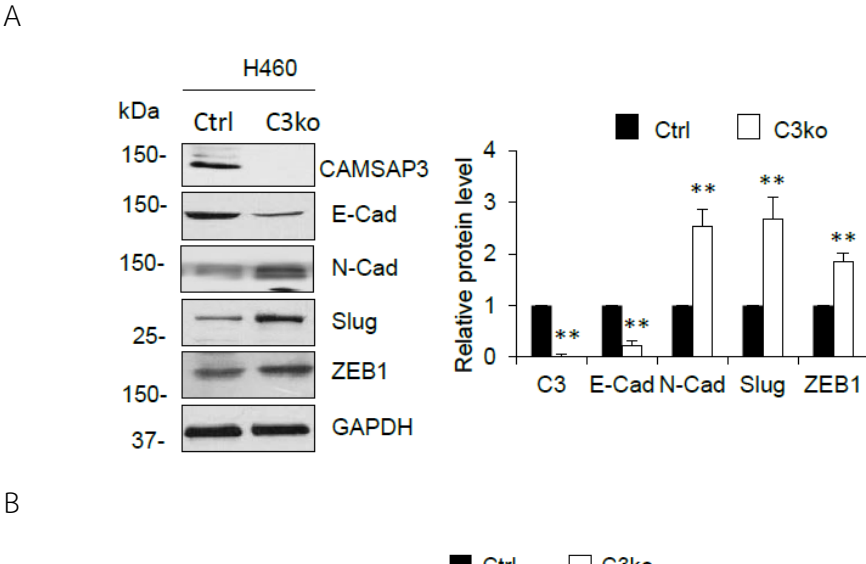


Figure 3 A. The sgRNA design schematic shows the target sequences of sgRNA#1 and #2 on *Camsap3* gene. B. A representative sequence of the *Camsap3* gene in H460/Ctrl and H460/C3ko cells.



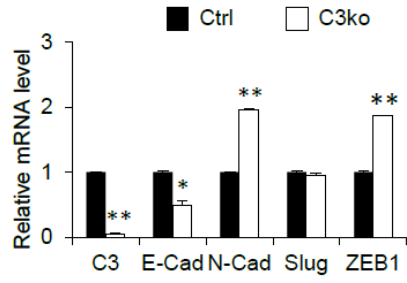


Figure 4 CAMSAP3 depletion mediated the epithelial-to-mesenchymal transition. A. CAMSAP3 was knocked out (C3ko) in H460 cells by the CRISPR-Cas9 system and analyzed for the level of CAMSAP3 and EMT markers. One representative immunoblot from three experiments is shown. Bar is the mean \pm SEM from triplicated experiments. **, P < 0.01 vs control cells. B. The mRNA expression levels of *CAMSAP3* and EMT markers were quantified by quantitative RT-PCR. Data are the mean \pm SEM from triplicated experiments. *, P < 0.05; **, P < 0.01 vs control cells.

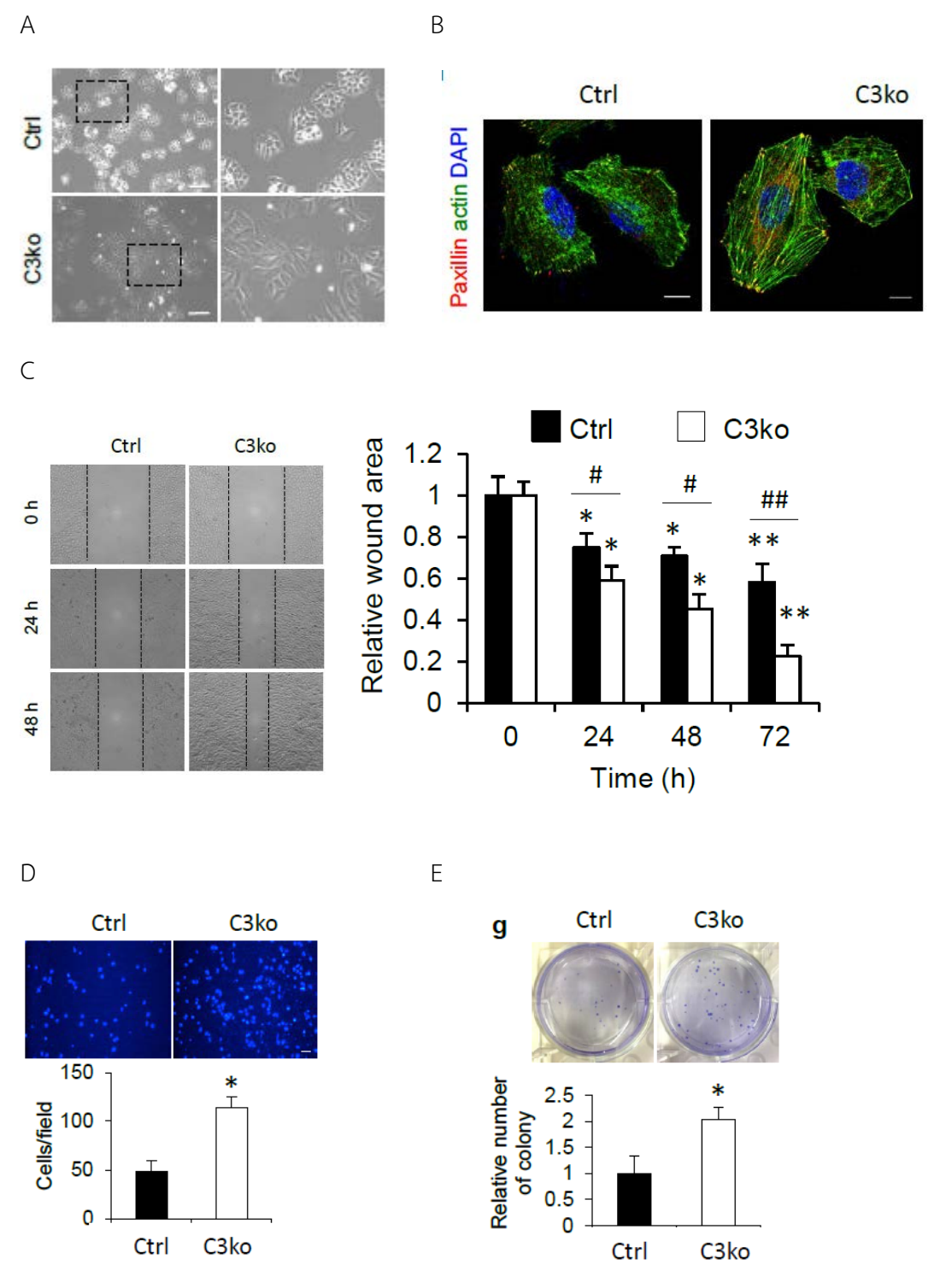


Figure 5 A. Images representing the morphology of *CAMSAP3*-knockout (H460/C3ko) and control (H460/Ctrl) H460 cells. (Scale bar 100 μ m) B. Immunofluorescence of paxillin (red), actin (green) and DAPI (blue) in H460/Ctrl and H460/C3ko cells. (Scale bar 10 μ m) C. Wound area was analyzed by wound healing migration assay in H460/Ctrl and H460/C3ko cells. Data are the mean \pm SEM from triplicate experiments. *, P < 0.05 vs time 0 h; $^{\#}$, P < 0.05 vs time 0 h; $^{\#}$, P < 0.05 vs time 0 h; $^{\#}$, P < 0.05 vs time 0 h; $^{\#}$, P < 0.05 vs time 0 h; $^{\#}$, P < 0.05 vs time 0 h; $^{\#}$, P < 0.05 vs time 0 h; $^{\#}$, P < 0.05 vs time 0 h; $^{\#}$, P < 0.05 vs time 0 h; $^{\#}$, P < 0.05 vs time 0 h; $^{\#}$, P < 0.05 vs time 0 h; $^{\#}$, P < 0.05 vs time 0 h; $^{\#}$, P < 0.05 vs time 0 h; $^{\#}$, P < 0.05 vs time 0 h; $^{\#}$, P < 0.05 vs time 0 h; $^{\#}$, P < 0.05 vs time 0 h; $^{\#}$, P < 0.05 vs time 0 h; $^{\#}$, P < 0.05 vs time 0 h; $^{\#}$, P < 0.05 vs time 0 h; $^{\#}$, P < 0.05 vs time 0 h; $^{\#}$, P < 0.05 vs time 0 h; $^{\#}$, P < 0.05 vs time 0 h; $^{\#}$, P < 0.05 vs time 0 h; $^{\#}$, P < 0.05 vs time 0 h; $^{\#}$, P < 0.05 vs time 0 h; $^{\#}$, P < 0.05 vs time 0 h; $^{\#}$, P < 0.05 vs time 0 h; $^{\#}$, $^{\#}$

0.05 and $^{\#}$, P < 0.01 vs control cells. D. The migrating cells were investigated by transwell migration assay. The image is representative of 5 fields/sample from triplicate experiments. E. Colony growth under detachment conditions was determined by soft agar assay in H460/Ctrl and H460/C3ko cells. The plot is the mean \pm SEM from triplicate experiments. *, P < 0.01 vs control cells.

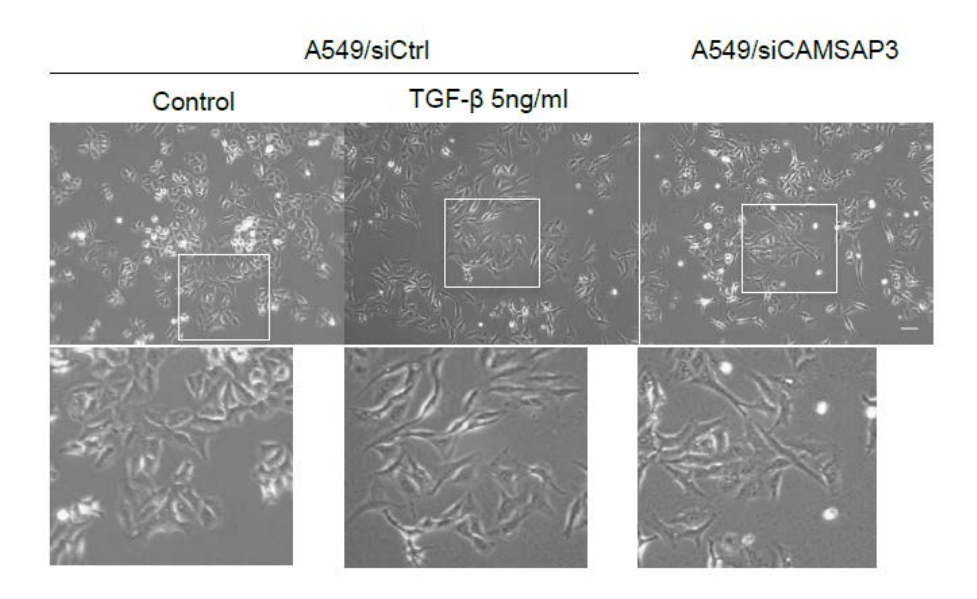


Figure 6 A549 cells were transfected with siRNA against CAMSAP3 or controls. The control-transfected cells were treated with or without TGF- β (5 ng/ml), and the images were captured after treatment for 48 h. (Scale bar 200 μ m).

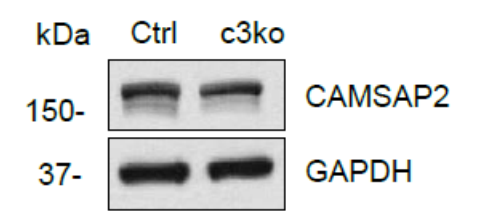


Figure 7 CAMSAP2 level in H460/Ctrl and H460/C3ko cells.

To strengthen this observation, we knocked down CAMSAP3 using specific siRNA in H460 and HeLa cells, and CAMSAP3 expression was shown to decrease upon this manipulation (Fig. 8A). Similar to the findings in *Camsap3* KO cells, cell motility and EMT marker expression were noticeably detected in both CAMSAP3 knockdown H460 and HeLa cells (Figs. 8B and C), suggesting that CAMSAP3 negatively regulates the transition of cells to mesenchymal-like phenotypes. We therefore utilized H460/ *Camsap3* KO cells as a principle model in the following studies.

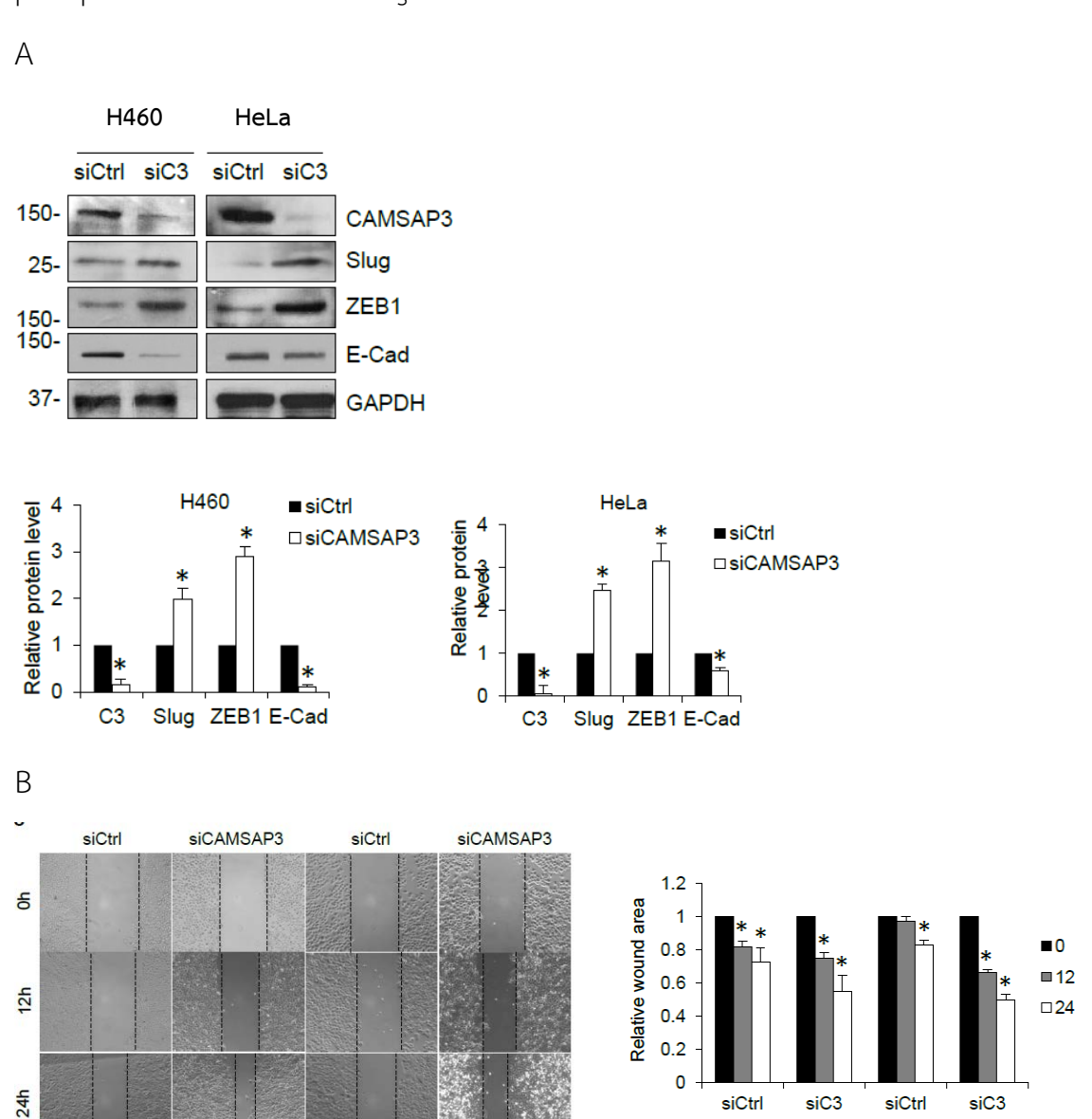


Figure 8 A. H460 and HeLa cells were transfected with siRNA to CAMSAP3. After 72 h, the cells were analyzed for CAMSAP3 and EMT marker expressions. The represented blot was from one of three experiments. Data are plotted as the mean \pm SEM. *, P < 0.01 vs control

H460

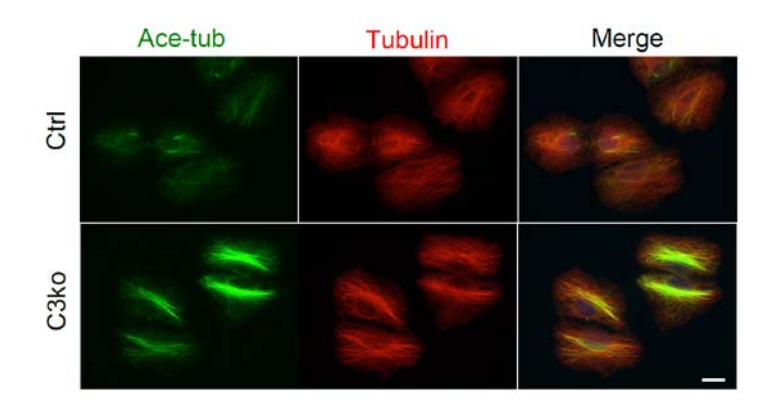
HeLa

transfected (siCtrl) cells. B. CAMSAP3-knockdown and control cells were subjected to wound healing assay. Wound area was presented as a relative value to the initial time point. Data are the mean \pm SEM from triplicated experiments. *, P < 0.05 vs time 0 h.

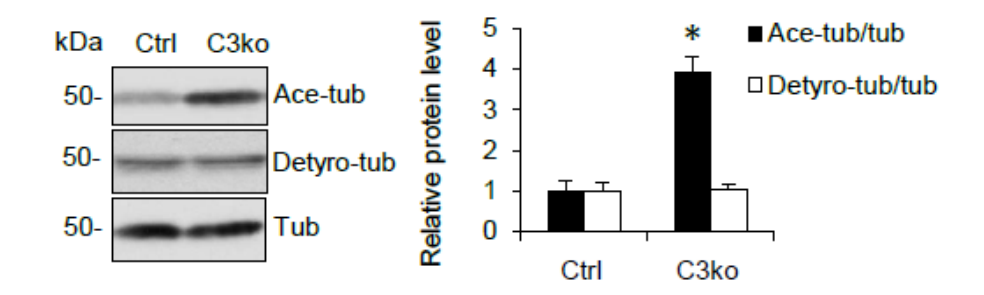
4. CAMSAP3 depletion enhances microtubule acetylation.

Microtubule architecture plays an important role in epithelial cell polarity (Toya et al., 2015), and the post-translation modification of tubulin, especially its acetylation, has been implicated in metastasis cancers (Boggs et al., 2015). We therefore examined the patterns of tubulin acetylation, a stable form of tubulin, in H460/Camsap3 KO cells. In comparison to control H460 cells, tubulin formed intense bundles and became more acetylated after Camsap3 removal (Fig. 9A). Western blotting also confirmed that in the absence of CAMSAP3, tubulin acetylation was substantially increased, consistent with previous reports (Tanaka et al., 2012). Meanwhile, the levels of total tubulin and detyrosinated tubulin were not altered (Fig. 9B). To further investigate the relevance of acetylated tubulin and cell migration activity, we evaluated the levels of this tubulin type among tested cell lines. As hypothesized, in H23 and H460 cells, which became more migratory and had relatively low CAMSAP3 levels, tubulin was more acetylated (Fig. 9C). In the other hand, HeLa cells, which have abundant CAMSAP3, had lower levels of this type of tubulin. These findings indicated that microtubule dynamics were altered in the absence of CAMSAP3, suggesting that CAMSAP3 could potentially attenuate cell motility through the suppression of excessive tubulin acetylation.





В



C

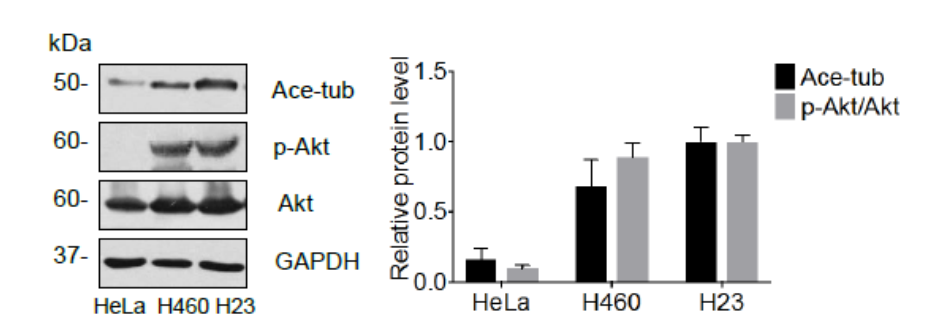


Figure 9 Tubulin acetylation was upregulated in the absence of *CAMSAP3*. A. Images represent double-staining for acetylated α-tubulin (green), α-tubulin (red) and DAPI (blue) in H460/Ctrl and H460/C3ko cells. B. The expression levels of tubulin acetylation and detyrosination were determined by immunoblotting in H460/Ctrl and H460/C3ko cells. Data are the mean \pm SEM from triplicate experiments. *, P < 0.01 vs control cells. C. Immunoblotting for acetylated tubulin (Ace-tub), Akt phosphorylation (p-Akt; S473), and Akt expression levels in HeLa, H460 and H23 cells. Data are the mean \pm SEM from triplicate experiments.

5. Protein kinase B (Akt) overactivation in the absence of CAMSAP3

Since protein kinase B (Akt) is widely known as a key player for the transition from an epithelial-to-mesenchymal phenotype, particularly in terms of cell migration (Xu, Yang and Lu, 2015), we next assessed the possible relation between CAMSAP3 and Akt regulation. Western blot analysis demonstrated that Akt became overactive, with an increase in phosphorylated Akt (p-Akt) in the CAMSAP3-depleted cells, whereas total Akt levels were not altered (Fig. 10A). Immunostaining experiments revealed that in the control cells, p-Akt staining exhibited distinct clusters located mainly in the cytoplasm. Intriguingly, compared to the control cells, the p-Akt in H460/Camsap3 KO cells had diffused throughout the cytoplasm, and a subpopulation was concentrated at the active edge of the cells (Fig. 10B). These data suggested that CAMSAP3 might normally act to suppress Akt activity.

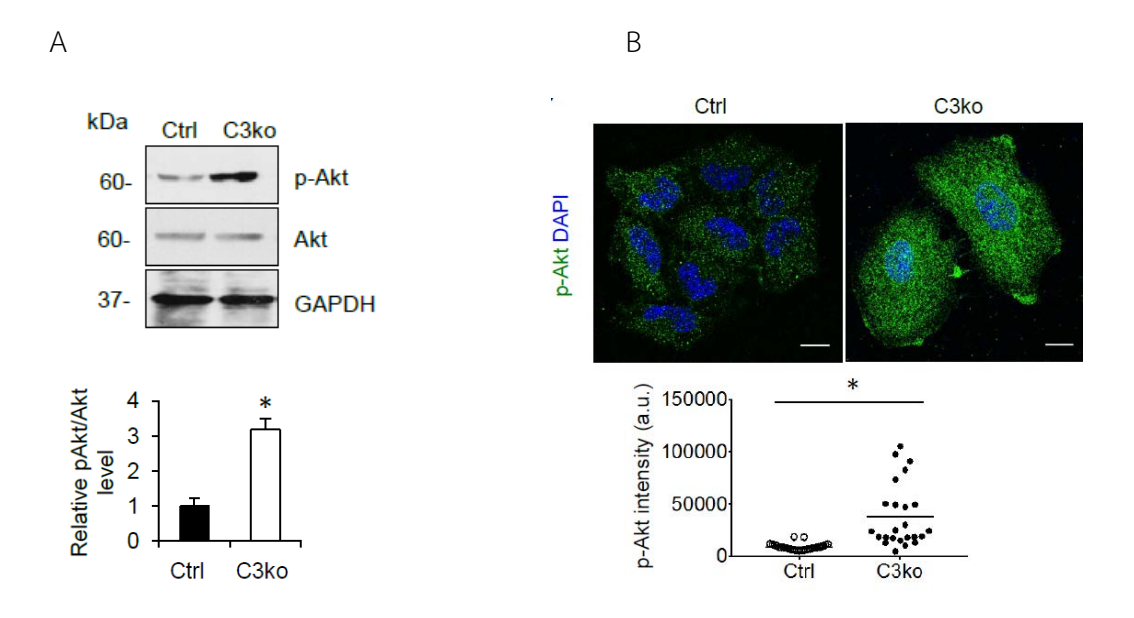


Figure 10 CAMSAP3 removal caused Akt overactivation. A. Akt phosphorylation and Akt levels in H460/Ctrl and H460/C3ko cells were examined by immunoblotting. Data are the mean \pm SEM from three experiments. *, P < 0.01 vs control cells. B. Images represent double-staining for p-Akt (green) and DAPI (blue) in H460/Ctrl and H460/C3ko cells. The fluorescence signal of p-Akt in 25 cells was quantified and presented. The bar represents the mean intensity of each group. *, P < 0.01 vs control cells. (Scale bar 10 μ m)

To support this observation, we treated H460/Camsap3 KO cells with LY294002, an Akt inhibitor, and their migratory behavior was examined. Wound scratch assays showed that attenuation of Akt activation by this treatment resulted in a reduction in migration rates, which corresponded to a decline in p-Akt levels (Figs. 11A and B). This finding led to the hypothesis that CAMSAP3 might interact with Akt and inhibit its activity. To verify this idea, we introduced exogenous His-tagged CAMSAP3 plasmids into H460 cells because of the lack of antibodies towards CAMSAP3 used in this study, and the cells were double-positive for endogenous Akt and CAMSAP3. The data showed that there are no overlapping signals between these two proteins (Fig. 12A). In addition, immunoprecipitation experiments demonstrated that co-precipitation of CAMSAP3 with either Akt or p-Akt was not significantly detected, indicating a lack of a physical interaction between the proteins (Fig. 12B). These findings suggest that CAMSAP3 might function as a suppressor of Akt phosphorylation without directly associating with it.

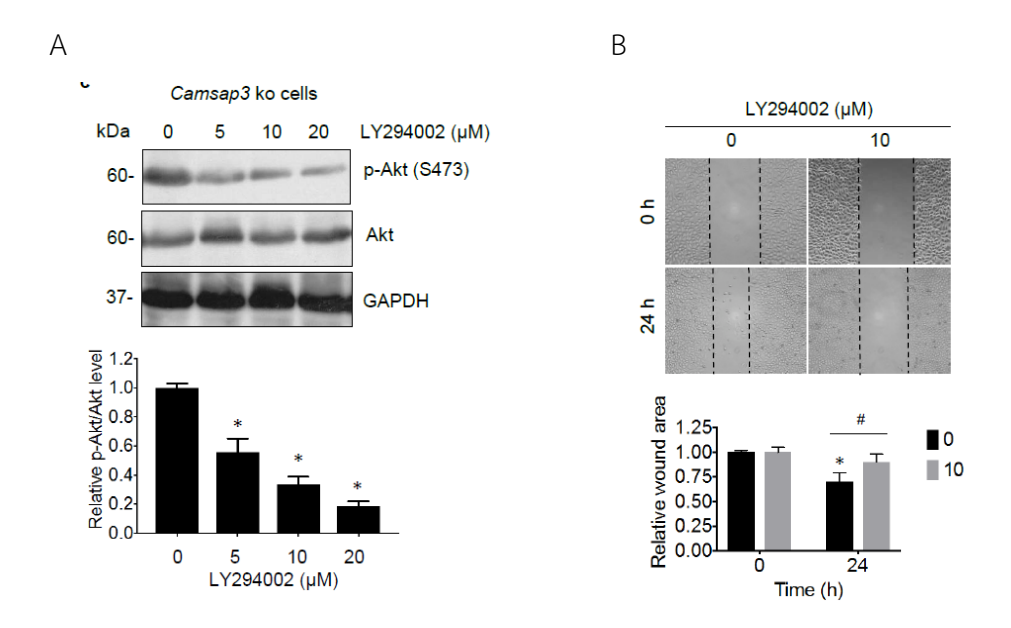


Figure 11 A. H460/C3ko cells were treated with LY294002 (0-20 μ M) for 14 h, and p-Akt and Akt levels were detected by immunoblotting. Data are the mean \pm SEM from triplicate experiments. *, P < 0.01 vs control cells. B. H460/C3ko cells were treated with LY294002 (10 μ M) or left untreated for 24 h and subjected to a wound healing migration assay.

Wound area was presented as a relative value to the initial time point. Data are the mean \pm SEM from triplicate experiments. *, P < 0.05 vs time 0 h; $^{\#}$, P < 0.05 vs H460/Ctrl cells.

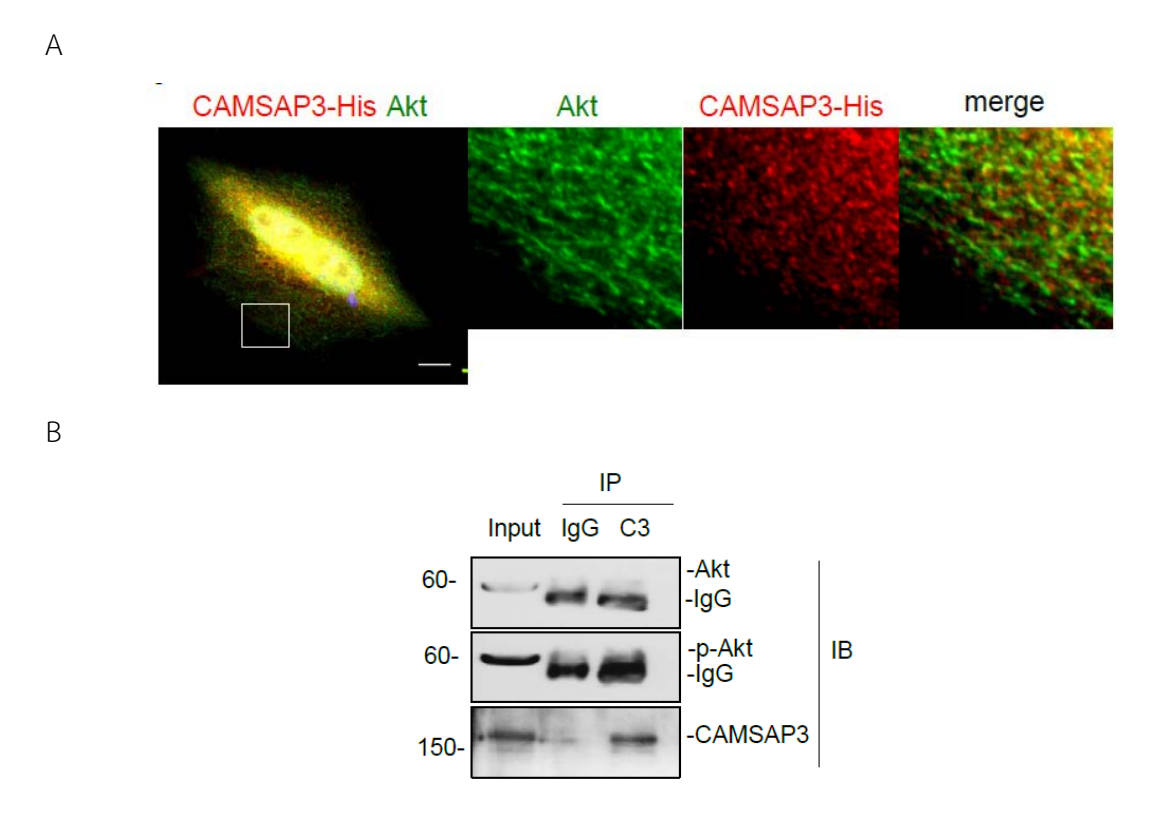


Figure 12 A. Immunofluorescence of exogenous CAMSAP3-His (red) and Akt (green) in H460 cells. (Scale bar 10 μ m). B. The interaction of CAMSAP3 with Akt or p-Akt was analyzed by immunoprecipitation assay. CAMSAP3 was pulled down with anti-CAMSAP3 antibody (IgG was used as a negative control) and then immunoblotted with anti-Akt or anti-p-Akt antibodies.

6. CAMSAP3 loss mediates Akt phosphorylation through a tubulin acetylation-dependent mechanism

Next, we investigated how CAMSAP3 negatively regulates Akt function. Since CAMSAP3 controls tubulin dynamics and acetylated tubulin has been reported to sustain Akt phosphorylation without stimulating its activity (Giustiniani *et al.*, 2009; Jo, Loison and Luo, 2014), we hypothesize that this tubulin post-translational modification may be involved in the CAMSAP3-Akt axis. To test this idea, we first examined the interaction between p-Akt and tubulin. A microtubule sedimentation assay was performed in H460

cells treated with taxol (a tubulin-stabilizing agent), nocodazole (a tubulin-depolymerizing agent), or DMSO, which served as a control. The results showed that the ratio of p-Akt in the insoluble portion to total p-Akt decreased after tubulin was depolymerized by nocodazole, a result that contrasted with those for the taxol-treated group (Fig. 13), confirming that phosphorylated Akt co-precipitated with tubulin.

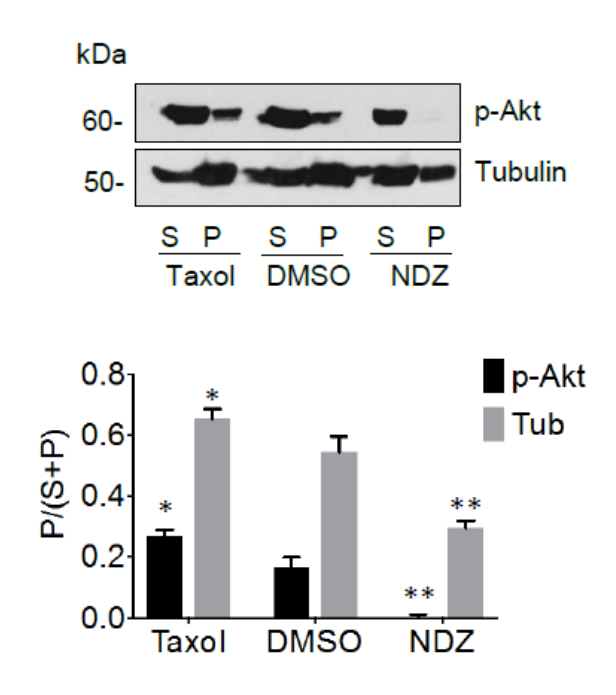
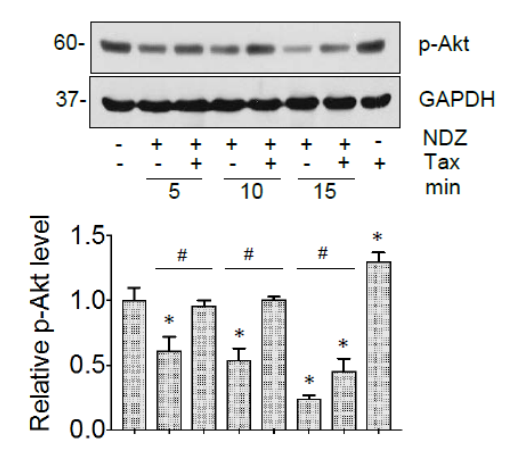


Figure 13 Tubulin hyperacetylation in *CAMSAP3* knockout cells promoted Akt function. H460 cells were treated with 1 μM taxol for 5 min at 37°C, 10 μM nocodazole (NDZ) for 1 h at 4°C, or DMSO. The lysate was separated into soluble (S) and pellet (P) fractions by microtubule sedimentation assay and analyzed for p-Akt and α -tubulin by immunoblotting. The ratio of pellet to total fraction was calculated and plotted as mean \pm SEM from triplicate experiments. *, P < 0.05; **, P < 0.01 vs DMSO-treated group.

Second, we tested whether tubulin polymerization was required to maintain Akt activation in this cell system. To this end, we treated H460 cells with nocodazole in the presence or absence of taxol for rescue experiments, and phosphorylated Akt levels were then examined. Western blotting revealed that the p-Akt level was significantly diminished following nocodazole washout, a change that was reversed when tubulin was repolymerized by taxol (Fig. 14A). This indicated that Akt activation was enhanced when

tubulin was stabilized. Immunostaining experiments also demonstrated that a subpopulation of p-Akt in the control cells was decorated with acetylated tubulin, a long-lasting tubulin form, which appeared to be enriched in H460/*Camsap3* KO cells with high acetylated tubulin levels (Fig. 14B).

Α





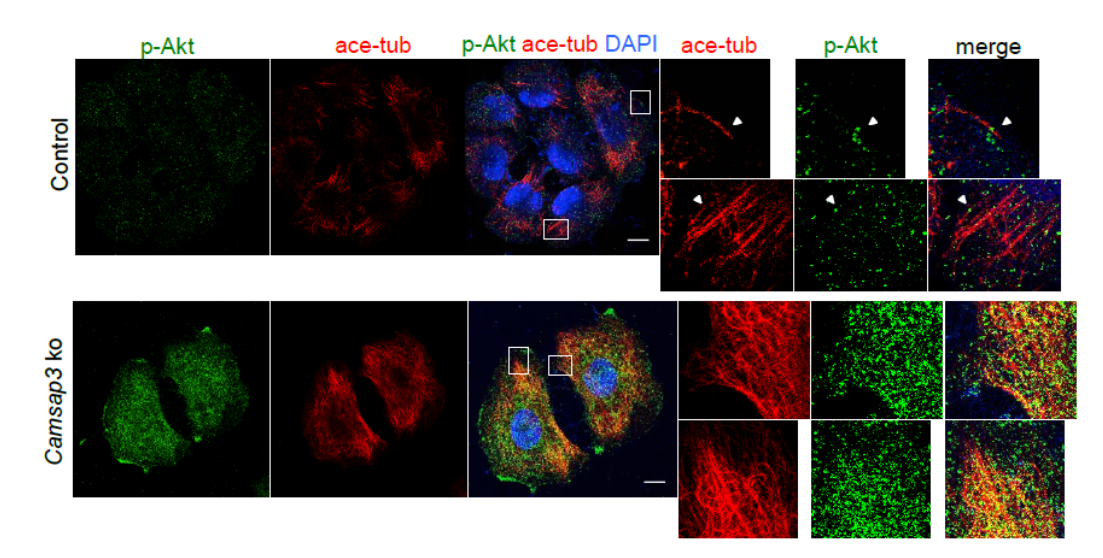


Figure 14 A. H460/C3ko cells were pretreated with 10 μM nocodazole (NDZ) at the indicated times, followed by incubation with or without 1 μM taxol (Tax) or DMSO, which served as a control, for 15 min. Western blotting was performed to analyze p-Akt, and GADPH served as a loading control. The represented blot was one of three experiments. Data are plotted as the mean \pm SEM. *, P < 0.01 vs DMSO treated group. #, P < 0.05 vs nocodazole-treated group. B. Immunofluorescence of p-Akt (green), acetylated tubulin (red) and DAPI (blue) in H460/ctrl and H460/C3ko cells. (Scale bar 10 μm).

To support this finding, we knocked down α -tubulin acetyltransferase 1 (α TAT1) using siRNA in H460/*Camsap3* KO cells since α TAT1 is an enzyme responsible for acetylation of tubulin at Lys40 (Chien *et al.*, 2016). Western blot analysis revealed that p-Akt levels were decreased following si- α TAT1 transfection (Fig. 15). However, we could not examine α TAT1 expression directly due to the lack of an available commercial antibody. Consistently, the p-Akt level was well-correlated with observed tubulin acetylation among tested cells (Fig. 9C). These observations suggested that CAMSAP3 loss caused a hyperactivation of Akt in an acetylated tubulin-dependent manner.

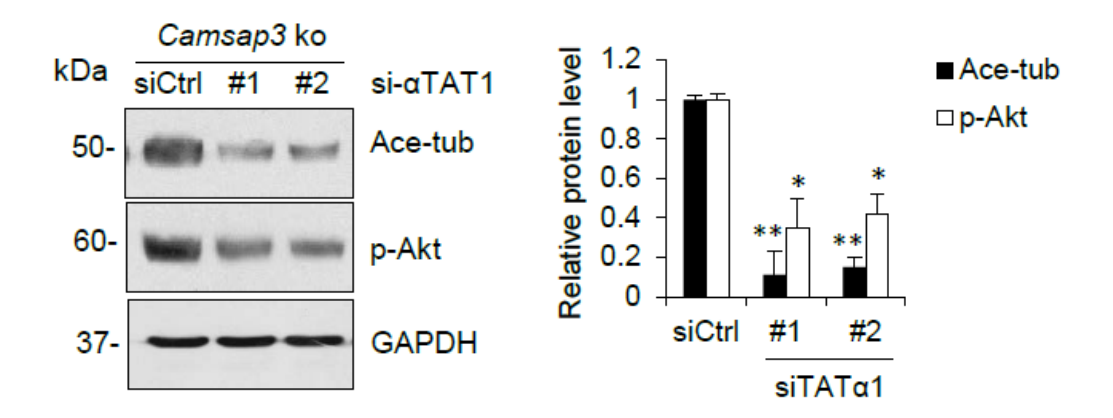


Figure 15 H460/C3ko cells were transfected with siRNA targeted to α-tubulin acetyltransferase 1 (si-αTAT1) and negative control siRNA. Acetylated tubulin (Ace-tub) and p-Akt were analyzed by immunoblotting in H460/C3ko transfected cells. The represented blot was from one of three experiments. Data are plotted as the mean \pm SEM. *, P < 0.05; ***, P < 0.01 vs control transfected H460/C3ko (siCtrl) cells.

7. Exogenous CAMSAP3 could reverse the mesenchymal characteristics mediated by CAMSAP3 knockdown.

To strengthen our observation, we stably introduced full-length CAMSAP3 (WT) in H460/Camsap3 KO cells, in which the endogenous and exogenous CAMSAP3 expression was elucidated (Fig. 16A). CAMSAP3-WT expression could reverse the phenotypic change after CAMSAP3 loss, and the cells began to appear as cluster of cobblestone-like cells, a native characteristic of H460 cells (Fig. 16B). Since our data indicated that CAMSAP3 functions to maintain normal Akt phosphorylation via modulation of tubulin dynamics, we next examined whether CAMSAP3-WT could rescue the perturbed kinase activity. Double-staining experiments showed that p-Akt strikingly disappeared following CAMSAP3-WT expression (Fig. 16C). Consistent with this observation, immunoblotting revealed that the upregulation of tubulin acetylation and phosphorylated Akt were attenuated in the presence of CAMSAP3-WT (Fig. 16D).

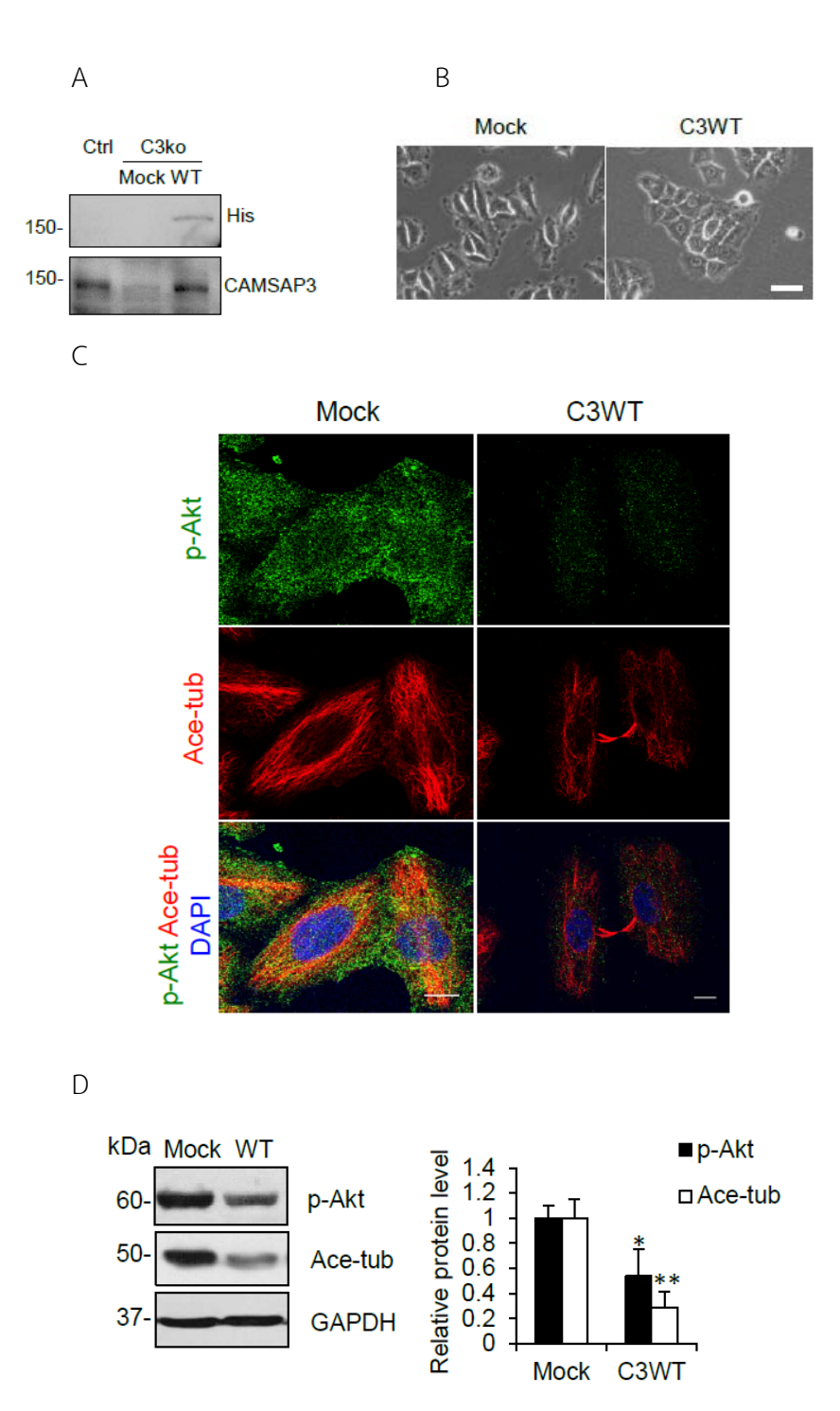


Figure 16 Full-length CAMSAP3 attenuated the upregulation of tubulin acetylation in H460/C3ko cells. A. Immunoblotting showed the expression of endogenous and exogenous CAMSAP3 in transfected cells. B. The morphology of H460/C3ko cells transfected with full-length CAMSAP3 (C3WT) and mock plasmids. (Scale bar 100 μ m) C. Immunofluorescence of p-Akt (green), acetylated tubulin (Ace-tub; red) and DAPI (blue) in H460/C3ko cells transfected with CAMSAP3-WT. (Scale bar 10 μ m) D. Acetylated tubulin

and p-Akt expression levels in response to CAMSAP3-WT transfection were determined by immunoblotting. The represented blot was from one of three experiments. Data are plotted as the mean \pm SEM. *, P < 0.01 vs mock transfected cells.

Based on our hypothesis that CAMSAP3 inhibited mesenchymal polarization, we tested whether the transfection of exogenous CAMSAP3-WT could suppress this phenotype, which was observed in H460/Camsap3 KO cells. Rescue experiments demonstrated that both the protein and mRNA expression levels of mesenchymal marker N-Cad was clearly downregulated in oppersite to epithelial marker E-Cad (Figs. 17A and B), as was the motile activity of H460/Camsap3 KO cells after the expression of CAMSAP3-WT (Fig. 17C). These findings supported the hypothesis that CAMSAP3 is essential to preserve epithelial polarization, preventing aberrant mesenchymal transformation from occurring.

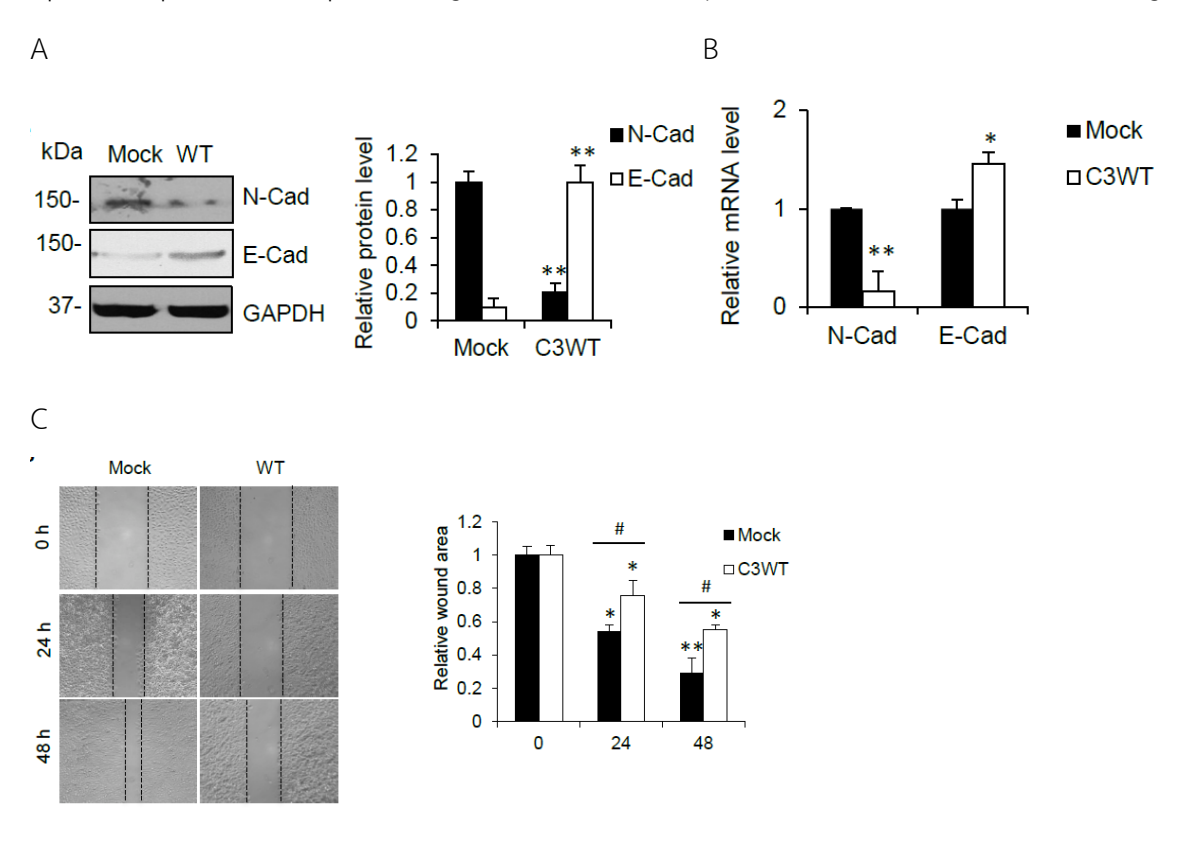


Figure 17 A. Protein and B. mRNA expressions of E-Cadherin (E-Cad) and N-Cadherin (N-Cad) in H460/C3ko cells transfected with CAMSAP3-WT and mock plasmids. Data are plotted as the mean \pm SEM. *, P < 0.05 and **, P < 0.01 vs mock transfected cells. C. The migration of H460/C3ko cells transfected with CAMSAP3 plasmids was analyzed by wound

healing/migration assay at the indicated time points. Data are presented as relative wound areas, and the mean \pm SEM was plotted. *, P < 0.05 and **, P < 0.01 vs time 0 h; $^{\#}$, P < 0.05 and $^{\#\#}$, P < 0.05 vs mock transfected cells.

8. CAMSAP2 might promote EMT, in opposite to CAMSAP3

The effect of CAMSAP2 on the EMT process was further evaluated. CAMSAP2 was knockdown in H460 cells using RNA interference, and protein expression in corresponding to siRNA was confirmed the knockdown efficiency (Fig. 18A). Wound healing assay demonstrated that CAMSAP2 knockdown exhibit slower cell migration rate compared to the control cells. This data indicated that CAMSAP2 might normally function to exert the transition of epithelial to mesenchymal phenotype. Interestingly, CAMSAP2 and CAMSAP3 have distinct role in the regulation of EMT. However, the molecular mechanism underlying CAMSAPs function is of great interested for further identification.

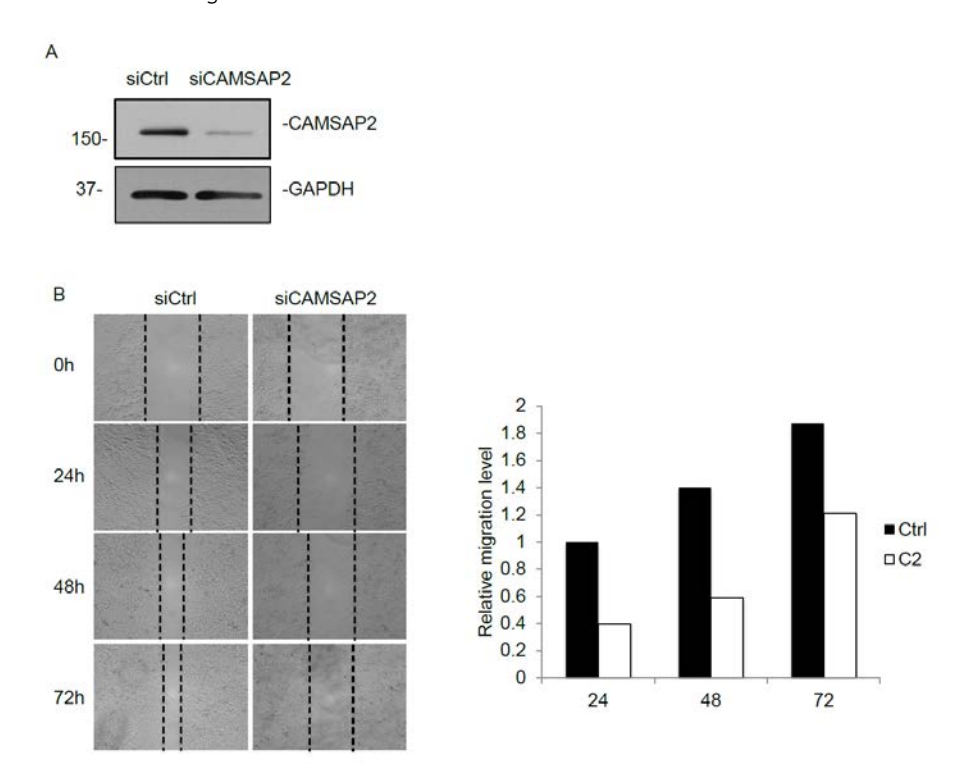


Figure 18 Effect of CAMSAP2 on cell migration. A. H460 cells were transfected with siRNA against CAMSAP2. CAMSAP2 expression was evaluated by Immunoblotting. B. Cell migration of CAMSAP2 knockdown and control cells were evaluated by wound healing migration assay.

Conclusion and Discussion

Our study demonstrated a distinctive function for CAMSAP3 in the regulation of EMT phenotypes. First, CAMSAP3 expression gradually decreased following TGF- β treatment, indicating that CAMSAP3 participated in this cellular process as a down-stream effector. Second, the absence of CAMSAP3 caused these morphological changes along with the upregulation of EMT markers. Thus, CAMSAP3 plays a negative role in the establishment of this mesenchymal-like behavior; therefore, its depletion facilitates cell locomotion. Finally, CAMSAP3 maintains normal microtubule dynamics, and tubulin became more stabilized or acetylated after CAMSAP3 removal. As a consequence of tubulin hyperacetylation, the activity of Akt was significantly enhanced independent of a physical interaction with CAMSAP3. This indicated that CAMSAP3 normally influences Akt activation via an alteration of tubulin stability.

Regarding our present data, we found a dependency of tubulin stability on CAMSAP3. Tubulin is a structural component of cells, and its dynamic properties are mainly regulated by post-translational modification. The acetylation of α -tubulin at lysine 40 and the removal of the C-terminus tyrosine (detyrosinated tubulin) are associated with more stable and long-lived microtubules, whereas the addition of tyrosine (tyrosinated tubulin) is linked with its depolymerization (Janke and Chloë Bulinski, 2011). The morphological changes caused by post-translational alterations contribute to certain cell activities, including cell mobilization (Etienne-Manneville, 2013). Tubulin-binding proteins, including CAMSAP family proteins, have been shown to be important modulators of this tubulin dynamic. We found that CAMSAP3 removal in H460 cells caused an increase in tubulin acetylation and enhanced front-rear cell mobility, a finding consistent with previous studies suggesting that tubulin stability was altered upon CAMSAP loss. Colon tissues display an apical-basal polarity, in which non-centrosomal microtubules become dominant and are oriented perpendicularly. Loss of CAMSAP3 interfered with their cell polarity and caused a loss of normal architecture (Toya *et al.*, 2015). Recent evidence has

also demonstrated that knock-down of CAMSAP2 and/or 3 in Caco2 cells, where CAMSAP2 and CAMSAP3 are abundant, led to the upregulation of acetylated and detyrosinated tubulins (Tanaka *et al.*, 2012). However, in U2OS cells, in the absence of CAMSAP2, detyrosinated microtubule levels were diminished, and cell polarity failed to develop (Jiang *et al.*, 2014). This finding contrasted with those in Caco2 cells. The diverse effects of CAMSAPs among cell types might depend on the proportions of tubulin types, the orientation of tubulin, the entire post-translational modification state of tubulin, or CAMSAP expression in specific cell types. The question of why polymerized tubulin levels is increased following CAMSAP3 depletion still needs to be clarified by future studies.

How does microtubule stability govern cell movement machinery? The cooperation of cytoskeletal elements is fundamentally important for this activity. Actin filaments, initiated from G-actin, promote the formation of lamellipodia at the leading edge and consequently interact with proteins related to cell contraction, such as myosin, which provides the pulling force to move forward (Asthana et al., 2013). Under the same circumstances, tubulin serves as a protrusion-supporting apparatus, allowing cellular traffic and signal transduction. A recent study showed that acetylation of tubulin was relevant to the metastatic potential of breast cancer (Boggs et al., 2015). The formation of a microtentacle structure, a microtubule-based protrusion, requires tubulin polymerization to generate physical force in cooperation with other cytoskeletal components and thus extend the cells to nearby tissue (Matrone et al., 2010). Importantly, tubulin acetylation was found to be enriched at the leading edge of the migrating cells (Palazzo et al., 2004; Yadav, Puri and Linstedt, 2009). Similarly, our study demonstrated that the level of global tubulin acetylation displayed a tight correlation to cellular locomotion. This indicated that tubulin modification serves a positive role in cell motility, in addition to its classical function as a marker of tubulin longevity.

Similar the emerging role of tubulin as a trafficking platform for intracellular molecules, it participates closely with actin to promote certain cell morphologies by being

involved in the translocation of protrusion components to actin elements (Akhshi, Wernike and Piekny, 2014). It has been reported that cytoplasmic linker protein-170 (CLIP-170), a microtubule plus-end-binding protein, interacts with Rac-1, a lamellipodia formation-regulatory protein, and that hepatocyte growth factor (HGF) caused the dissociation of this complex, leading to lamellipodia formation and cell migration (Suzuki and Takahashi, 2008). Likewise, CAMSAP3 has been demonstrated to govern actin organization via GEF-H1, a guanine nucleotide exchange effector that is responsible for small Rho GTPase activation. The modification of tubulin dynamics to a stable phase, mediated by CAMSAP3 loss, led to the upregulation of GEF-H1 and, subsequently, the formation of actin stress fibers (Nagae, Meng and Takeichi, 2013). The present study also found that in the absence of CAMSAP3, actin filaments were assembled along with an increase in paxillin, a focal adhesion protein. This might be related to tubulin stabilization in CAMSAP-depleted states. The particular events that interfered with tubulin dynamics might influence such effectors and thus influence cellular activity.

Since tubulins behave as an amplifier of signal transduction, the activation state of several signaling molecules, including protein kinase B (Akt), is exerted by their interaction with tubulin. The Akt signaling pathway is of paramount importance in several sporadic cancers since it is a potential target for anticancer drug development (Altomare and Testa, 2005). In light of the multiple effects of Akt, it is very clear that EMT regulatory proteins are targets of the Akt signaling pathway (Suman *et al.*, 2014; Xu, Yang and Lu, 2015). Phosphorylation of Akt at serine 473 and threonine 308 by an upstream phosphatidylinositol 3-kinase (PI3K) initiated its activity; however, the sustained nature of its activated state has shed light on the regulation of signal transduction. Emerging evidence shows that there is an association between tubulin and Akt activation. Specifically, the evidence shows that tubulin is required to prolong Akt stimulation. Our data demonstrated that an increase in acetylated tubulin, mediated by CAMSAP3 depletion, led to the upregulation of Akt phosphorylation, despite a lack of cytological colocalization of CAMSAP3 and Akt. This aberrant phosphorylation was, in turn, diminished

by either α TAT1 siRNA or tubulin destabilizing agents, indicating a noticeable influence of tubulin on Akt function. This is similar to previous studies, in which it was reported that tubulin stabilization by acetylation is essential to sustain Akt action but is not involved with its signal generation (Giustiniani *et al.*, 2009; Kunoh *et al.*, 2010; Jo, Loison and Luo, 2014). Our observation therefore provides evidence of the remarkable function of CAMSAP3 in Akt signaling via a tubulin acetylation-dependent mechanism, highlighting the cooperation between these proteins that influences cell behavior.

Output (Acknowledge the Thailand Research Fund)

International Journal Publications (see Appendix)

- 1) Unahabhokha T, Chanvorachote P, Sritularak B, Kitsongsermthon J, <u>Pongrakhananon V</u>. Gigantol inhibits epithelial to mesenchymal process in human lung cancer cells. Evidence-based Complementary and Alternative Medicines. (2016); 2016: 4561674.
- 2) Treesuwan S, Sritularak B, Chanvorachote P, <u>Pongrakhananon V.</u> Cypripedin diminishes an epithelial-to-mesenchymal transition in non-small cell lung cancer cells through suppression of Akt/GSK-3β signalling. Scientific Reports. (2018) Submitted.
- 3) <u>Pongrakhananon V</u>, Wattanathamasan O, Takeichi M, Chetprayoon C, Chanvorachote P. CAMSAP3, a microtubule minus-end binding protein, negatively regulates epithelial to mesenchymal transition via modification of the tubulin dynamics-Akt machinery. Journal of Cell Science. (2018) Submitted.

Research Utilization and Application

Topic: Structure of cell and organelle functions
 Course: Human Cellular Physiology (Undergraduate and graduated class)
 Faculty of Pharmaceutical Sciences, Chulalongkorn Unoversity

Others e.g. national journal publication, proceeding, international conference, book chapter, patent

- Pongrakhananon V. Role of calmodulin-regulated spectrin associated protein on cellular polarity. German-Thai Cancer Research Symposium 2017 "Highlight into molecular biology of cancer and targeted molecules" April 19th, 2017. Faculty of Pharmaceutical Sciences, Chulalonkorn University (Invited speaker)
- 2) <u>Pongrakhananon V</u>, Unahabhokha T_, and Chanvorachote P. CAMSAP3, a tubulin minus-end binding protein, attenuates epithelial to mesenchymal transition and alters microtubule stabilization in lung cancer. TRF-OHEC Annual Congress 2018. January 10-12, 2018. The Regent Chaam Beach Resort, Phetchaburi. (Poster presentation) (see Appendix)

- 3) <u>Pongrakhananon V</u>. Emerging role of tubulin in cancer metastasis. 34th International Annual Meeting in Pharmaceutical Sciences and 2nd CU FPhS -RIKEN CDB Symposium "Advances in Cellular and Molecular Biology" March 8-9, 2018 Anoma Grand Hotel, Bangkok. (Invited speaker)
- 4) Pongrakhananon V, Wattanathamsan O and Takeichi M. CAMSAP3, a tubulin minusend binding protein, attenuates epithelial to mesenchymal transition and alters microtubule dynamic in non-small cell lung cancer. American Association for Cancer Research (AACR) Annual Meeting. April 14-18, 2018. Chicago, USA. (Poster presentation) (see Appendix)

References

Akhmanova, A. and Hoogenraad, C. C. (2015) 'Microtubule Minus-End-Targeting Proteins', *Current Biology*, 25(4), pp. R162–R171. doi: 10.1016/j.cub.2014.12.027.

Akhshi, T. K., Wernike, D. and Piekny, A. (2014) 'Microtubules and actin crosstalk in cell migration and division', *Cytoskeleton*, 71(1), pp. 1–23. doi: 10.1002/cm.21150.

Aktas, B. *et al.* (2009) 'Stem cell and epithelial-mesenchymal transition markers are frequently overexpressed in circulating tumor cells of metastatic breast cancer patients', *Breast Cancer Research*, 11(4), p. R46. doi: 10.1186/bcr2333.

Altomare, D. A. and Testa, J. R. (2005) 'Perturbations of the AKT signaling pathway in human cancer', *Oncogene*. Nature Publishing Group, 24(50), pp. 7455–7464. doi: 10.1038/sj.onc.1209085.

Asthana, J. *et al.* (2013) 'Inhibition of HDAC6 Deacetylase Activity Increases Its Binding with Microtubules and Suppresses Microtubule Dynamic Instability in MCF-7 Cells * **S. doi:** 10.1074/jbc.M113.489328.

Boggs, A. E. *et al.* (2015) '\$**α\$**-Tubulin acetylation elevated in metastatic and basal-like breast cancer cells promotes microtentacle formation, adhesion, and invasive migration.', *Cancer research*. American Association for Cancer Research, 75(1), pp. 203–215. doi: 10.1158/0008-5472.CAN-13-3563.

Bolós, V. *et al.* (2003) 'The transcription factor Slug represses E-cadherin expression and induces epithelial to mesenchymal transitions: a comparison with Snail and E47 repressors.', *Journal of cell science*, 116(Pt 3), pp. 499–511. Available at: http://www.ncbi.nlm.nih.gov/pubmed/12508111 (Accessed: 11 December 2017).

Burridge, K. and Guilluy, C. (2016) 'Focal adhesions, stress fibers and mechanical tension.', *Experimental cell research*. NIH Public Access, 343(1), pp. 14–20. doi: 10.1016/j.yexcr.2015.10.029.

Cao, Y.-W. et al. (2015) 'Implications of the Notch1-Snail/Slug-epithelial to mesenchymal transition axis for lymph node metastasis in infiltrating ductal carcinoma', *The Kaohsiung*

Journal of Medical Sciences, 31(2), pp. 70-76. doi: 10.1016/j.kjms.2014.11.008.

Chanvorachote, P., Pongrakhananon, V. and Chaotham, C. (2016) 'Roles of nitric oxide on cancer stemness and metastasis in lung cancer cells', *Asian Journal of Pharmaceutical Sciences*, 11(1). doi: 10.1016/j.ajps.2015.10.017.

Chanvorachote, P., Pongrakhananon, V. and Chunhacha, P. (2014) 'Prolonged nitric oxide exposure enhances anoikis resistance and migration through epithelial-mesenchymal transition and caveolin-1 upregulation', *BioMed Research International*, 2014. doi: 10.1155/2014/941359.

Chaotham, C. *et al.* (2014) 'A bibenzyl from Dendrobium ellipsophyllum inhibits epithelial-to-mesenchymal transition and sensitizes lung cancer cells to anoikis', *Anticancer Research*, 34(4).

Chien, J.-Y. et al. (2016) 'a TAT1 downeglation induces mitatic catastrophe in Helaard A549 cells', Cell Death Discovery, 2, p. 16006. doi: 10.1038/cddiscovery.2016.6.

Etienne-Manneville, S. (2013) 'Microtubules in Cell Migration', *Annual Review of Cell and Developmental Biology*, 29(1), pp. 471–499. doi: 10.1146/annurev-cellbio-101011-155711.

Frisch, S. M., Schaller, M. and Cieply, B. (2013) 'Mechanisms that link the oncogenic epithelial-mesenchymal transition to suppression of anoikis.', *Journal of cell science*. Company of Biologists, 126(Pt 1), pp. 21–9. doi: 10.1242/jcs.120907.

Ganguly, A. *et al.* (2012) 'The Role of Microtubules and Their Dynamics in Cell Migration', *Journal of Biological Chemistry*, 287(52), pp. 43359–43369. doi: 10.1074/jbc.M112.423905.

Giustiniani, J. *et al.* (2009) 'Tubulin acetylation favors Hsp90 recruitment to microtubules and stimulates the signaling function of the Hsp90 clients Akt / PKB and p53', *Cellular Signalling*. Elsevier Inc., 21(4), pp. 529–539. doi: 10.1016/j.cellsig.2008.12.004.

Gravdal, K. *et al.* (2007) 'A switch from E-cadherin to N-cadherin expression indicates epithelial to mesenchymal transition and is of strong and independent importance for the progress of prostate cancer.', *Clinical cancer research [: an official journal of the American Association for Cancer Research*, 13(23), pp. 7003–11. doi: 10.1158/1078-

0432.CCR-07-1263.

Guadamillas, M. C., Cerezo, A. and Del Pozo, M. A. (2011) 'Overcoming anoikis--pathways to anchorage-independent growth in cancer.', *Journal of cell science*. The Company of Biologists Ltd, 124(Pt 19), pp. 3189–97. doi: 10.1242/jcs.072165.

Hanahan, D. and Weinberg, R. A. (2011) 'Hallmarks of Cancer: The Next Generation', *Cell*, 144(5), pp. 646–674. doi: 10.1016/j.cell.2011.02.013.

Heerboth, S. et al. (2015) 'EMT and tumor metastasis.', Clinical and translational medicine. Springer, 4, p. 6. doi: 10.1186/s40169-015-0048-3.

Hendershott, M. C. and Vale, R. D. (2014) 'Regulation of microtubule minus-end dynamics by CAMSAPs and Patronin', 2014. doi: 10.1073/pnas.1404133111.

Holz, C. *et al.* (2011) 'Epithelial–mesenchymal-transition induced by EGFR activation interferes with cell migration and response to irradiation and cetuximab in head and neck cancer cells', *Radiotherapy and Oncology*, 101(1), pp. 158–164. doi: 10.1016/j.radonc.2011.05.042.

Hulit, J. *et al.* (2007) 'N-Cadherin Signaling Potentiates Mammary Tumor Metastasis via Enhanced Extracellular Signal-Regulated Kinase Activation', *Cancer Research*, 67(7), pp. 3106–3116. doi: 10.1158/0008-5472.CAN-06-3401.

Iwatsuki, M. *et al.* (2010) 'Epithelial-mesenchymal transition in cancer development and its clinical significance', *Cancer Science*, 101(2), pp. 293–299. doi: 10.1111/j.1349-7006.2009.01419.x.

Janke, C. and Chloë Bulinski, J. (2011) 'Post-translational regulation of the microtubule cytoskeleton: mechanisms and functions', *Nature Reviews Molecular Cell Biology*. Nature Publishing Group, 12(12), pp. 773–786. doi: 10.1038/nrm3227.

Jiang, K. *et al.* (2014) 'Microtubule Minus-End Stabilization by Polymerization-Driven CAMSAP Deposition', *Developmental Cell*, 28, pp. 295–309. doi: 10.1016/j.devcel.2014.01.001.

Jiang, K. and Akhmanova, A. (2011) 'Microtubule tip-interacting proteins: a view from both

ends', Current Opinion in Cell Biology, 23(1), pp. 94-101. doi: 10.1016/j.ceb.2010.08.008.

Jo, H., Loison, F. and Luo, H. R. (2014) 'Microtubule dynamics regulates Akt signaling via dynactin p150', *Cellular Signalling*. Elsevier Inc., 26(8), pp. 1707–1716. doi: 10.1016/j.cellsig.2014.04.007.

Kaverina, I. and Straube, A. (2011) 'Regulation of cell migration by dynamic microtubules.', *Seminars in cell & developmental biology*. NIH Public Access, 22(9), pp. 968–74. doi: 10.1016/j.semcdb.2011.09.017.

Kunoh, T. *et al.* (2010) 'A Novel Human Dynactin-Associated Protein , dynAP , Promotes Activation of Akt , and Ergosterol-Related Compounds Induce dynAP-Dependent Apoptosis of Human Cancer Cells', 9(November), pp. 2934–2943. doi: 10.1158/1535-7163.MCT-10-0730.

Lade-Keller, J. et al. (2013) 'E- to N-cadherin switch in melanoma is associated with decreased expression of phosphatase and tensin homolog and cancer progression.', *The British journal of dermatology*, 169(3), pp. 618–28. doi: 10.1111/bjd.12426.

Matrone, M. A. *et al.* (2010) 'Metastatic breast tumors express increased tau, which promotes microtentacle formation and the reattachment of detached breast tumor cells', *Oncogene*, 29(22), pp. 3217–3227. doi: 10.1038/onc.2010.68.

Mendez, M. G., Kojima, S. I. and Goldman, R. D. (2010) 'Vimentin induces changes in cell shape, motility, and adhesion during the epithelial to mesenchymal transition', *The FASEB Journal*, 24(6), pp. 1838–1851. doi: 10.1096/fj.09-151639.

Nagae, S., Meng, W. and Takeichi, M. (2013) 'Non-centrosomal microtubules regulate F-actin organization through the suppression of GEF-H1 activity', *Genes to Cells*, 18(5), pp. 387–396. doi: 10.1111/gtc.12044.

Palazzo, A. F. *et al.* (2004) 'Localized Stabilization of Microtubules by Integrin- and FAK-Facilitated Rho Signaling', *Science*, 303(5659), pp. 836–839. doi: 10.1126/science.1091325.

Palmer, T. D. *et al.* (2011) 'Targeting tumor cell motility to prevent metastasis', *Advanced Drug Delivery Reviews*, 63(8), pp. 568–581. doi: 10.1016/j.addr.2011.04.008.

Pasquier, E. and Kavallaris, M. (2008) 'Microtubules: A dynamic target in cancer therapy', *IUBMB Life*. Wiley Subscription Services, Inc., a Wiley company, 60(3), pp. 165–170. doi: 10.1002/iub.25.

Perdiz, D. *et al.* (2011) 'The ins and outs of tubulin acetylation: More than just a post-translational modification?', *Cellular Signalling*. Pergamon, 23(5), pp. 763–771. doi: 10.1016/J.CELLSIG.2010.10.014.

Ran, F. A. *et al.* (2013) 'Genome engineering using the CRISPR-Cas9 system', *Nat. Protocols*, 8(11), pp. 2281–2308. doi:

10.1038/nprot.2013.143\rhttp://www.nature.com/nprot/journal/v8/n11/abs/nprot.2013.143. html#supplementary-information.

Shih, J.-Y. and Yang, P.-C. (2011) 'The EMT regulator slug and lung carcinogenesis', *Carcinogenesis*, 32(9), pp. 1299–1304. doi: 10.1093/carcin/bgr110.

Siegel, R. L., Miller, K. D. and Jemal, A. (2015) 'Cancer statistics, 2015', *CA: A Cancer Journal for Clinicians*, 65(1), pp. 5–29. doi: 10.3322/caac.21254.

Spaderna, S. *et al.* (2006) 'A Transient, EMT-Linked Loss of Basement Membranes Indicates Metastasis and Poor Survival in Colorectal Cancer', *Gastroenterology*, 131(3), pp. 830–840. doi: 10.1053/j.gastro.2006.06.016.

Suman, S. *et al.* (2014) 'Activation of AKT signaling promotes epithelial-mesenchymal transition and tumor growth in colorectal cancer cells', *Molecular Carcinogenesis*, 53(S1), pp. E151–E160. doi: 10.1002/mc.22076.

Suzuki, K. and Takahashi, K. (2008) 'Regulation of lamellipodia formation and cell invasion by CLIP-170 in invasive human breast cancer cells', *Biochemical and Biophysical Research Communications*, 368(2), pp. 199–204. doi: 10.1016/j.bbrc.2008.01.069.

Tanaka, N. *et al.* (2012) 'Nezha / CAMSAP3 and CAMSAP2 cooperate in epithelial-speci fi c organization of noncentrosomal microtubules', 109(49). doi: 10.1073/pnas.1218017109.

Torre, L. A. *et al.* (2015) 'Global cancer statistics, 2012', *CA: A Cancer Journal for Clinicians*, 65(2), pp. 87–108. doi: 10.3322/caac.21262.

Toya, M. et al. (2015) 'CAMSAP3 orients the apical-to-basal polarity of microtubule arrays in epithelial cells', pp. 1–6. doi: 10.1073/pnas.1520638113.

Uchikado, Y. *et al.* (2005) 'Slug Expression in the E-cadherin preserved tumors is related to prognosis in patients with esophageal squamous cell carcinoma.', *Clinical cancer research: an official journal of the American Association for Cancer Research*, 11(3), pp. 1174–80. Available at: http://www.ncbi.nlm.nih.gov/pubmed/15709186 (Accessed: 11 December 2017).

Unahabhokha, T., Chanvorachote, P. and Pongrakhananon, V. (2016) 'The attenuation of epithelial to mesenchymal transition and induction of anoikis by gigantol in human lung cancer H460 cells', *Tumor Biology*, 37(7), pp. 8633–8641. doi: 10.1007/s13277-015-4717-z.

Wheelock, M. J. et al. (2008) 'Cadherin switching'. doi: 10.1242/jcs.000455.

Xu, W., Yang, Z. and Lu, N. (2015) 'A new role for the PI3K/Akt signaling pathway in the epithelial-mesenchymal transition', *Cell Adhesion & Migration*, 9(4), pp. 317–324. doi: 10.1080/19336918.2015.1016686.

Yadav, S., Puri, S. and Linstedt, A. D. (2009) 'A Primary Role for Golgi Positioning in Directed Secretion, Cell Polarity, and Wound Healing', *Molecular Biology of the Cell*, 20, pp. 1728–1736. doi: 10.1091/mbc.E08.

Yang, H. *et al.* (2015) 'TGF- **N**-Lactivated SMAD3/4 complex transcriptionally upregulates N-cadherin expression in non-small cell lung cancer', *Lung Cancer*, 87, pp. 249–257. doi: 10.1016/j.lungcan.2014.12.015.

Yilmaz, M. and Christofori, G. (2009) 'EMT, the cytoskeleton, and cancer cell invasion.', *Cancer metastasis reviews*, 28(1–2), pp. 15–33. doi: 10.1007/s10555-008-9169-0.

Zhang, X. *et al.* (2013) 'N-Cadherin Expression Is Associated with Acquisition of EMT Phenotype and with Enhanced Invasion in Erlotinib-Resistant Lung Cancer Cell Lines', *PLoS ONE*. Edited by R. Rota. Public Library of Science, 8(3), p. e57692. doi: 10.1371/journal.pone.0057692.

Hindawi Publishing Corporation Evidence-Based Complementary and Alternative Medicine Volume 2016, Article ID 4561674, 10 pages http://dx.doi.org/10.1155/2016/4561674

Research Article

Gigantol Inhibits Epithelial to Mesenchymal Process in Human Lung Cancer Cells

Thitita Unahabhokha,¹ Pithi Chanvorachote,¹,² Boonchoo Sritularak,³ Jutarat Kitsongsermthon,⁴ and Varisa Pongrakhananon¹,²

- ¹Cell-Based Drug and Health Product Development Research Unit, Faculty of Pharmaceutical Sciences, Chulalongkorn University, Bangkok 10330, Thailand
- ²Department of Pharmacology and Physiology, Faculty of Pharmaceutical Sciences, Chulalongkorn University, Bangkok 10330, Thailand
- ³Department of Pharmacognosy and Pharmaceutical Botany, Faculty of Pharmaceutical Sciences, Chulalongkorn University, Bangkok 10330, Thailand
- ⁴Department of Pharmaceutics and Industrial Pharmacy, Faculty of Pharmaceutical Sciences, Chulalongkorn University, Bangkok 10330, Thailand

Correspondence should be addressed to Varisa Pongrakhananon; varisa.p@pharm.chula.ac.th

Received 31 May 2016; Revised 11 July 2016; Accepted 1 August 2016

Academic Editor: Yoshiki Mukudai

Copyright © 2016 Thitita Unahabhokha et al. This is an open access article distributed under the Creative Commons Attribution License, which permits unrestricted use, distribution, and reproduction in any medium, provided the original work is properly cited.

Lung cancer remains a leading public health problem as evidenced by its increasing death rate. The main cause of death in lung cancer patients is cancer metastasis. The metastatic behavior of lung cancer cells becomes enhanced when cancer cells undergo epithelial to mesenchymal transition (EMT). Gigantol, a bibenzyl compound extracted from the Thai orchid, *Dendrobium draconis*, has been shown to have promising therapeutic potential against cancer cells, which leads to the hypothesis that gigantol may be able to inhibit the fundamental EMT process in cancer cells. This study has demonstrated for the first time that gigantol possesses the ability to suppress EMT in non-small cell lung cancer H460 cells. Western blot analysis has revealed that gigantol attenuates the activity of ATP-dependent tyrosine kinase (AKT), thereby inhibiting the expression of the major EMT transcription factor, Slug, by both decreasing its transcription and increasing its degradation. The inhibitory effects of gigantol on EMT result in a decrease in the level of migration in H460 lung cancer cells. The results of this study emphasize the potential of gigantol for further development against lung cancer metastasis.

1. Introduction

Epithelial to mesenchymal transition (EMT) is the hallmark of cancer metastasis [1–3]. According to several reports, the survival rate of lung cancer patients is significantly diminished upon the diagnosis of cancer metastasis [4–6]. The development of a compound with the potential to attenuate the EMT process has been gaining interest in pharmaceutical research as a potential anticancer treatment. The change of cancer cells from epithelial to mesenchymal phenotypes facilitates the aggressiveness of the cancer. Several proteins have been identified as markers of the transdifferentiation process [7]. Decreases in E-cadherin, a transmembrane

protein responsible for intercellular interactions, have been reported during the transition into the mesenchymal phenotype [7–9]. On the other hand, N-cadherin is a cell-cell adhesion molecule in mesenchymal cells. The EMT process is characterized by a shift in expression from E-cadherin to N-cadherin [10, 11]. Likewise, it has been claimed that Vimentin, another protein necessary for the motility of the mesenchymal cells, is increased during the EMT process [12]. These changes in molecular expression are mainly driven by the Snail family of transcription factors, in particular Slug [13, 14]. The Slug expression is further regulated through transcription and degradation pathways. β -catenin is responsible for interacting with the transcriptional factor Slug and promotes

FIGURE 1: Chemical structure of gigantol.

the production of Slug at the level of DNA. Conversely, its stability is controlled by GSK-3 β , which causes ubiquitination and degradation of Slug [1–3, 15–17]. Recent evidence has suggested that AKT is able to influence the activity of both β -catenin and GSK-3 β [4–6, 12, 15, 17]. An increase in AKT activity is also associated with EMT incidence in cancer cells [7, 18]. Taken together, these molecular pathways have an important role in the induction of cancer cells towards EMT. Alterations of the activity or expression of these molecules could potentially prevent cancer metastasis.

Several pure compound extractions from Thai medicinal orchids, including gigantol, have been reported to have promising anticancer activity [18–23]. Gigantol (Figure 1) is a stilbenoid derivative isolated from the stem of *Dendrobium draconis*, a Thai medicinal orchid [10, 11, 24]. The anticancer activity of gigantol has been widely reported [12, 18–20]; however, its effect on EMT inhibition and the underlying mechanisms have yet to be clarified. It is possible that gigantol may have the potential to attenuate the regulatory mechanisms of EMT, leading to a decrease in aggressive cancer cell behavior. This result would support the development of this compound for cancer therapy.

2. Materials and Methods

2.1. Materials. Gigantol was isolated from Dendrobium draconis as previously described [23]. Gigantol used in this study was isolated from the dried powdered stems of D. draconis and extracted by MeOH using vacuum-liquid chromatography (VLC) and column chromatography (CC) with more than 95% purity. Gigantol was prepared in dimethyl sulfoxide (DMSO) for stock solution and PBS (phosphatebuffered saline) was used to dilute the stock solution into working concentrations. The final concentration of DMSO used in all of the experiments was 0.1%. The results from the treatment groups were compared with the untreated control exposed to the 0.1% final concentration of DMSO. DMSO, 3-(4,5-dimethylthiazol-2-yl)-2,5-diphenyltetrazolium bromide (MTT), Hoechst 33342, propidium iodide (PI), bovine serum albumin (BSA), and antibody for ubiquitin were purchased from Sigma Chemical, Inc. (St. Louis, MO, USA). Antibodies for Rho GTP and Rac GTP were purchased from NewEaszt Bioscience (King of Prussia, PA, USA). Antibodies for N-cadherin, E-cadherin, Vimentin, Snail, ZEB-1, Slug, β -catenin, phosphorylated AKT (Ser473), AKT, phosphorylated GSK-3 β (Ser9), GSK-3 β , GAPDH, and peroxidaseconjugated secondary antibodies were purchased from Cell Signaling (Danvers, MA, USA).

2.2. Cell Culture. Human non-small cell lung cancer cells (NCI-H460) were obtained from the American Type Culture Collection (ATCC, Manassas, VA, USA) and cultured in Roswell Park Memorial Institute (RPMI) 1640 medium supplemented with 10% fetal bovine serum (FBS), 2 mM L-glutamine, 100 U/mL penicillin, and 100 μ g/mL streptomycin. Cells were cultured at 37°C in a humidified incubator with 5% CO₂ and passaged at near confluence with trypsin-EDTA. RPMI 1640 medium, FBS, L-glutamine, penicillin, streptomycin, PBS, trypsin, and EDTA were purchased from GIBCO (Grand Island, NY, USA).

2.3. Cytotoxic Assay. Cell viability was examined using a colorimetric 3-(4,5-dimethylthiazol-2-yl)-2,5-diphenyltetrazolium bromide (MTT) assay. H460 cells were seeded in 96-well plates at 10,000 cells/well and incubated overnight at 37°C. After being exposed to gigantol treatments at various doses (0–50 μ M) for 24 h, the medium was removed and 100 μ L of MTT solution was added to each well. Then the plates were further incubated for 4 h at 37°C. After that the medium was replaced by 100 μ L of DMSO to dissolve the formazan crystal. The intensity of formazan produce was measured at 570 nm using a microplate reader (Anthros, Durham, NC, USA). Cell viability was presented as percentage from the absorbance of the treatment groups in relative to the control group.

2.4. Apoptosis Assay. Apoptotic and necrotic cells were identified using a fluorescent nuclear staining dye, Hoechst 33342, and PI. H460 cells were seeded in 96-well plates at 10,000 cells/well and incubated overnight at $37^{\circ}\mathrm{C}$. After exposing to gigantol treatments at various doses (0–50 $\mu\mathrm{M}$) for 24 h, cells were washed and incubated with 10 $\mu\mathrm{g/mL}$ Hoechst 33342 and 5 $\mu\mathrm{g/mL}$ PI for 30 min in the dark. Nuclei condensation and DNA fragmentation of apoptotic and necrotic cells were observed and scored using fluorescence microcopy (Olympus IX51 with DP70). The data were presented as percentage from the number of apoptotic and necrotic cells of the treatment groups relative to the control group.

2.5. Migration Assay. Cell migration was observed using wound healing and transwell migration assay. H460 cells were treated with gigantol at noncytotoxic concentrations for 24 h before subjecting to migration evaluation. For wound healing assay, treated H460 cells were seeded in 24-well plates at 250,000 cells/well and incubated overnight at 37°C. After monolayer of cells was formed, a micropipette tip was used to create a wound space. Then the cell debris was removed by washing with PBS and replaced with serum-free culture medium. The cell migration level across the wounded space was observed and evaluated using inverted microscope (Olympus IX51 with DP70). The relative migration level was calculated from the difference of the wound space between the treatment group and the control group divided by the wound space of the control group at each evaluation time. For transwell migration assay, the treated H460 cells were seeded at 25,000 cells/well into the upper chamber of 24transwell plates in a serum-free culture medium while culture medium with 10% FBS was added to the lower chamber.

After incubating at 37° C for 24 h, the leftover cells on the upper chamber were removed and the migrated cells in the lower chamber were stained with $10 \,\mu\text{g/mL}$ Hoechst 33342 for 30 min in the dark. The Hoechst staining cells were photographed and analyzed using fluorescence microcopy (Olympus IX51 with DP70).

2.6. Invasion Assay. Cell invasion was evaluated using transwell invasion assay. H460 cells were treated with gigantol at noncytotoxic concentrations for 24 h before subjecting to invasion evaluation. Before the experiment, 0.5% of matrigel was coated on the filter membrane of the transwell chamber and left overnight at 37°C. Then, the treated H460 cells were seeded at 25,000 cells/well into the upper chamber of 24-transwell plates in a serum-free culture medium while culture medium with 10% FBS was added to the lower chamber. After incubating at 37°C for 24 h, the noninvaded cells in the upper chamber were removed and the invaded cells in the lower chamber were stained with 10 μ g/mL Hoechst 33342 for 30 min in the dark. The Hoechst staining cells were photographed and analyzed using fluorescence microcopy (Olympus IX51 with DP70).

2.7. Western Blot Analysis. Levels of protein expression were evaluated using Western blot analysis. H460 cells were exposed to treatment of gigantol at noncytotoxic concentrations. After specific treatments, cells were harvested by washing twice with cold PBS and incubated with lysis buffer containing 20 mM Tris-HCl (pH 7.5), 1% Triton X-100, 150 mM sodium chloride, 10% glycerol, 1 mM sodium orthovanadate, 50 mM sodium fluoride, 100 mM phenylmethylsulfonyl fluoride, and protease inhibitor cocktail for 1 h at 4°C. The cell lysate was collected as protein sample and subjected to protein concentration measurement using the BCA assay kit (Bio-Rad Laboratories, Hercules, CA, USA). Protein from each sample was denatured by heating at 95°C for 5 min with Laemmli loading buffer prior to the gel electrophoresis. Then protein samples were separated by molecular weight using precast 5-10% gradient SDS-PAGE gel and transferred to nitrocellulose membranes. After blocking with 5% skim milk for 1 h, the membranes were incubated with the indicated primary antibodies at 4°C overnight. After that, the membranes were washed thoroughly with TBST (25 mM Tris-HCl (pH 7.5), 125 mM NaCl, and 0.05% Tween 20), and then they were incubated with horseradish peroxide-conjugated secondary antibodies for an additional hour at room temperature. Subsequently, the bands were then visualized using a film exposure with a chemiluminescence detection system and quantified using analyst/PC densitometry software by Image J.

2.8. Immunoprecipitation Assay. Levels of protein interaction were evaluated using immunoprecipitation assay. In order to detect the ubiquitin-protein complex, lactacystin was pretreated to the cells an hour prior to gigantol treatment. After specific treatments, cells were harvested and lysed with lysis buffer. Then the cell lysate was separated and collected by centrifuging at 12,000 rpm for 3 min at 4°C before preclearing with agarose bead for 45 min at 4°C to prevent unspecific binding. The remaining cell lysate was subjected to protein

measurement for equal loading. Next the anti-Slug antibody was added to the cleared lysate and incubated overnight at 4°C before further adding agarose beads for an additional 2 h at 4°C. The precipitated immune complexes were washed with ice-cold lysis buffer, resuspended in 2x Laemmli sample buffer, and then heated at 95°C for 5 min. After that, immune complexes were separated using precast 5–10% gradient SDS-PAGE gel electrophoresis and transferred to nitrocellulose membranes; the Western blot analysis was then performed using an anti-ubiquitin antibody.

2.9. Statistical Analysis. Results were expressed as mean \pm standard error (SE) from at least four independently performed experiments. Differences between treatments were examined using the one-way analysis of variance (ANOVA) followed by *post hoc* test. p values less than 0.05 were considered statistically significant.

3. Results

3.1. Cytotoxicity of Gigantol on Lung Cancer H460 Cells. To determine the concentration of gigantol used in this study, we first evaluated the cytotoxicity of gigantol using MTT and apoptosis assays. Before cell viability evaluation, H460 cells were treated with various concentrations of gigantol (0–50 μ M) for 24 h. Figure 2(a) illustrates that, at concentrations lower than 50 μ M, there was no significant impact of gigantol on cell viability. The apoptosis assay confirmed that low concentrations of gigantol (0, 1, 5, 10, or 20 μ M) could not induce apoptosis in cells (Figure 2(b)). Approximately 15% of the cells treated with 50 μ M of gigantol showed signs of nuclear condensation, an indicator of apoptosis (Figure 2(c)). Noncytotoxic concentrations of gigantol (0–20 μ M) were used in subsequent experiments.

3.2. Gigantol Suppresses Epithelial to Mesenchymal Transition (EMT) in Lung Cancer H460 Cells. Cellular migration is an indicator of cells undergoing EMT; therefore, the migration levels of H460 were examined to determine the effect of gigantol on EMT inhibition. The H460 cells were pretreated with gigantol at 1, 5, 10, and $20 \,\mu\text{M}$ for 24 h, and then the migration level was assessed using wound healing and transwell migration assays. Figure 3(a) shows that treatment with 20 μ M gigantol suppressed cell migration across the wound space (approximately 70%) at intervals as early as 24 h. At 72 h, gigantol concentrations of 1, 5, 10, or $20 \,\mu\text{M}$ were able to significantly attenuate H460 cell motility when compared to the control. Consistently, results from the transwell migration assay demonstrated that gigantol was able to decrease the number of cells moving across the transwell filter within 24 h in a dose-dependent manner (Figure 3(b)). A similar trend was also observed in a transwell invasion assay. Approximately 30%, 35%, 45%, and 70% reductions in invasion were recorded in H460 cells treated for 24 h with concentrations of 1, 5, 10, and 20 µM of gigantol, respectively (Figure 3(c)). To evaluate migration activity at the molecular level, the expression levels of Rho GTP and Rac GTP in H460 cells were evaluated after 24 h of treatment with gigantol. Rho GTP is responsible for stress fiber extension, while Rac GTP

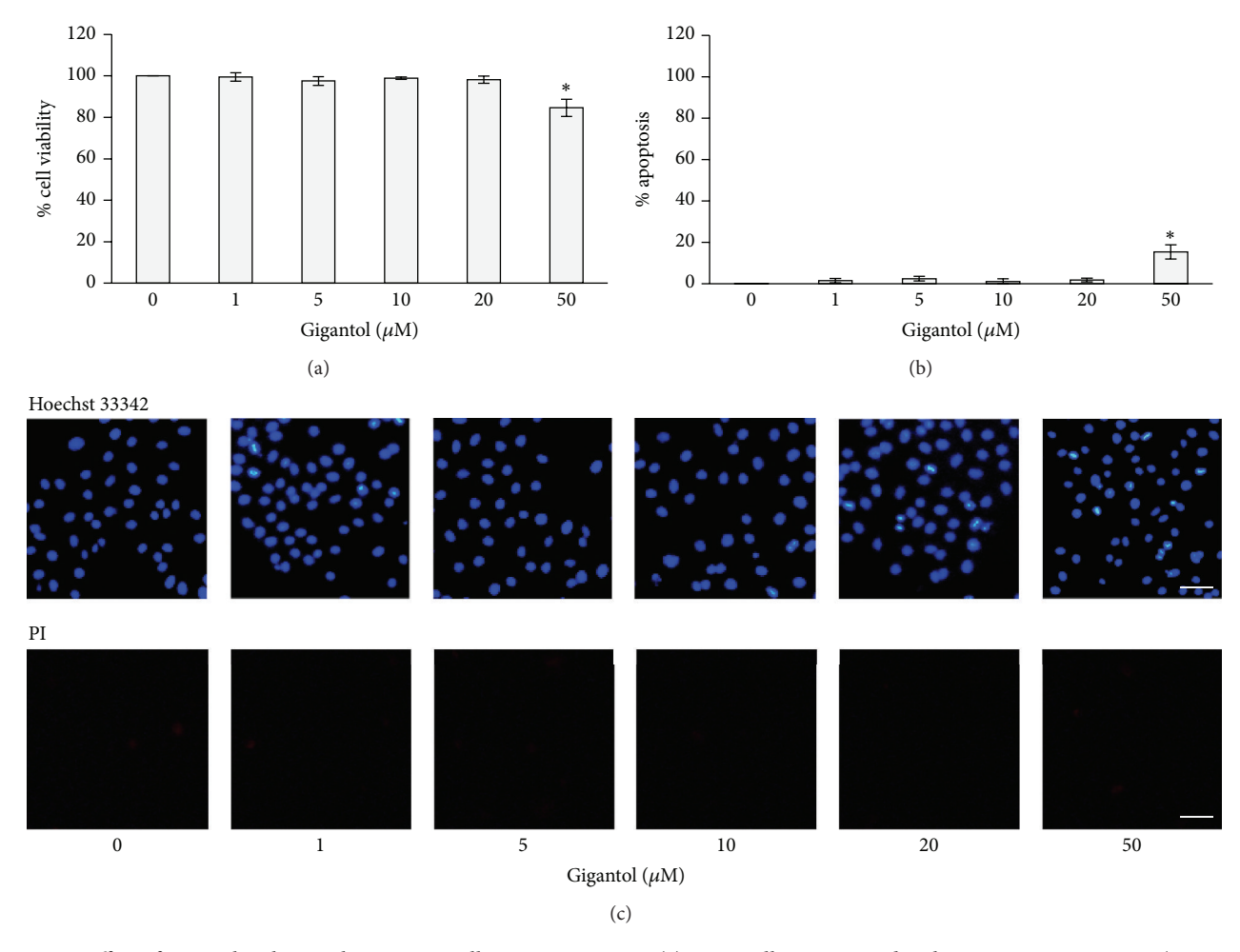


FIGURE 2: Effect of gigantol on human lung cancer cell H460 cytotoxicity. (a) H460 cells were treated with various concentrations (0–50 μ M) of gigantol for 24 h, and cell viability was measured by the MTT assay. The viability of untreated control cells was represented as 100%. (b) H460 cells were treated with various concentrations (0–50 μ M) of gigantol for 24 h, and apoptotic cell death was evaluated using Hoechst 33342 nuclear staining dye. The percentages of cells undergoing apoptosis were calculated comparing to the untreated control cells. (c) The fluorescence images were captured after staining with either Hoechst 33342 or propidium iodide (PI) (*scale bar* is 50 μ m). The data represent mean \pm SE (n = 4). *p < 0.05 versus untreated control cells.

regulates lamellipodia formation [25-27]. Both proteins are known migration regulator proteins that enhance cytoskeleton reorganization by facilitating membrane protrusion at the edges of the cell. The results from the Western blot analysis shown in Figure 3(d) demonstrate that treatment of gigantol suppressed Rho GTP and Rac GTP expression. To determine the existence of an association between gigantol and EMT, the expression of EMT marker proteins including E-cadherin, N-cadherin, Vimentin, Snail, Slug, and ZEB-1 was evaluated. The results from the Western blot analysis support our hypothesis that treatment with various concentrations of gigantol (0-20 μ M) for 24 h switched the cadherin type from E-cadherin to N-cadherin in the treated H460 cells (Figure 3(e)). In addition, 1, 5, 10, and 20 μ M of gigantol reduced Vimentin expression levels by 90%, 70% 50%, and 40%, respectively. Gigantol treatment also suppressed the expression levels of the Slug transcription factor, while Snail and ZEB-1 levels remained unchanged. This result suggests

that gigantol is able to inhibit the EMT process by decreasing the production of the EMT transcription factor Slug.

3.3. Gigantol Increases Ubiquitination of the Slug Transcription Factor. We have demonstrated that gigantol is able to down-regulate Slug expression. The objective of this experiment was to further investigate the mechanism by which gigantol treatment downregulates Slug expression. It was reported that the stability of Slug is controlled by proteasomal degradation [12, 28]. Protein degradation occurs either via proteasomal or via lysosomal pathways. To determine which pathway contributes to Slug downregulation, H460 cells were treated with either the proteasomal inhibitor lactacystin (Lac) or the lysosomal inhibitor concanamycin A (CMA). Figure 4(a) shows that Lac was able to inhibit the reduction of Slug in response to gigantol. This indicated that Slug degradation was blocked in proteasomal-suppressed cells resulting in an increased accumulation of Slug in the treated cells when compared to

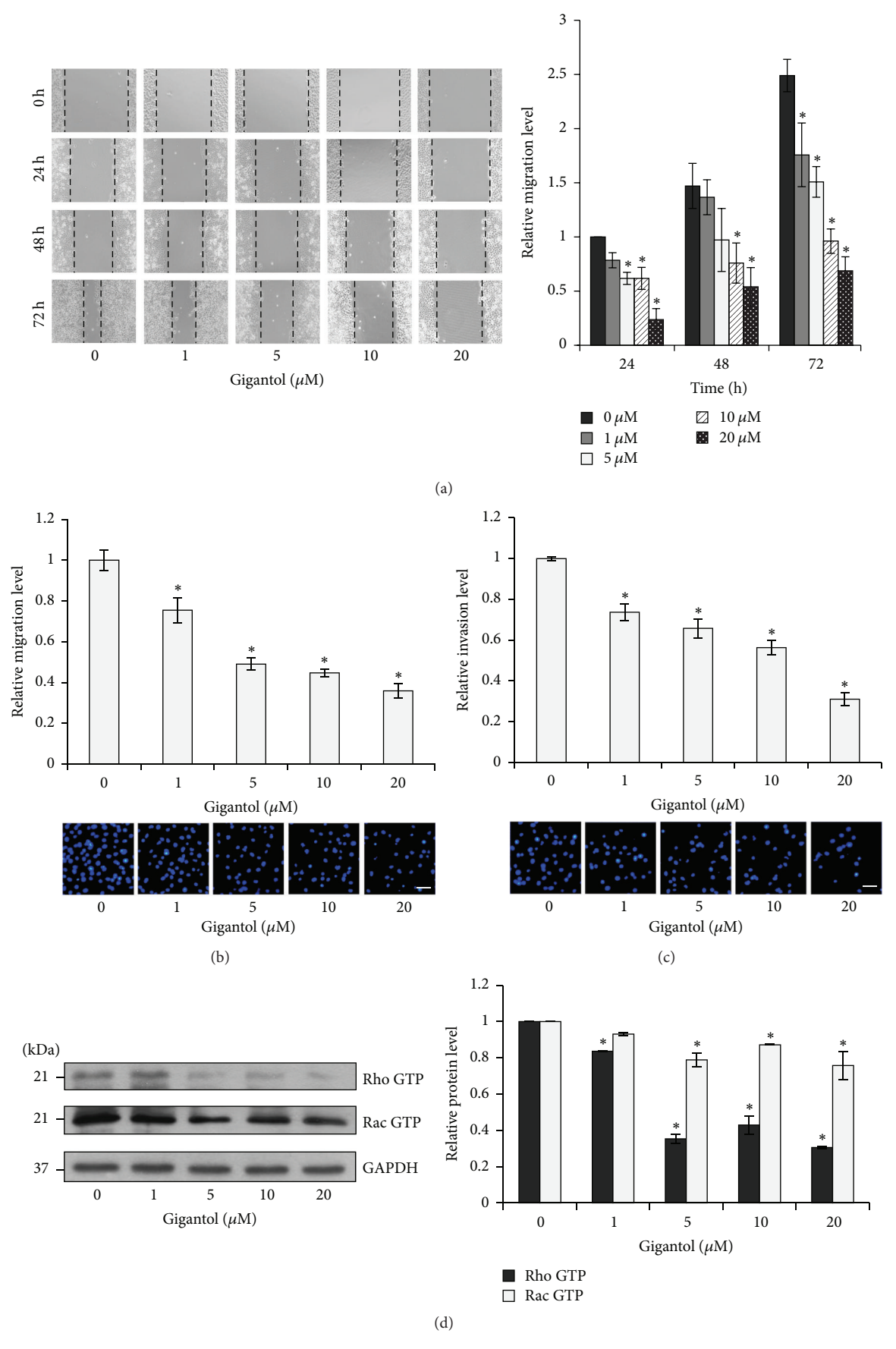


FIGURE 3: Continued.

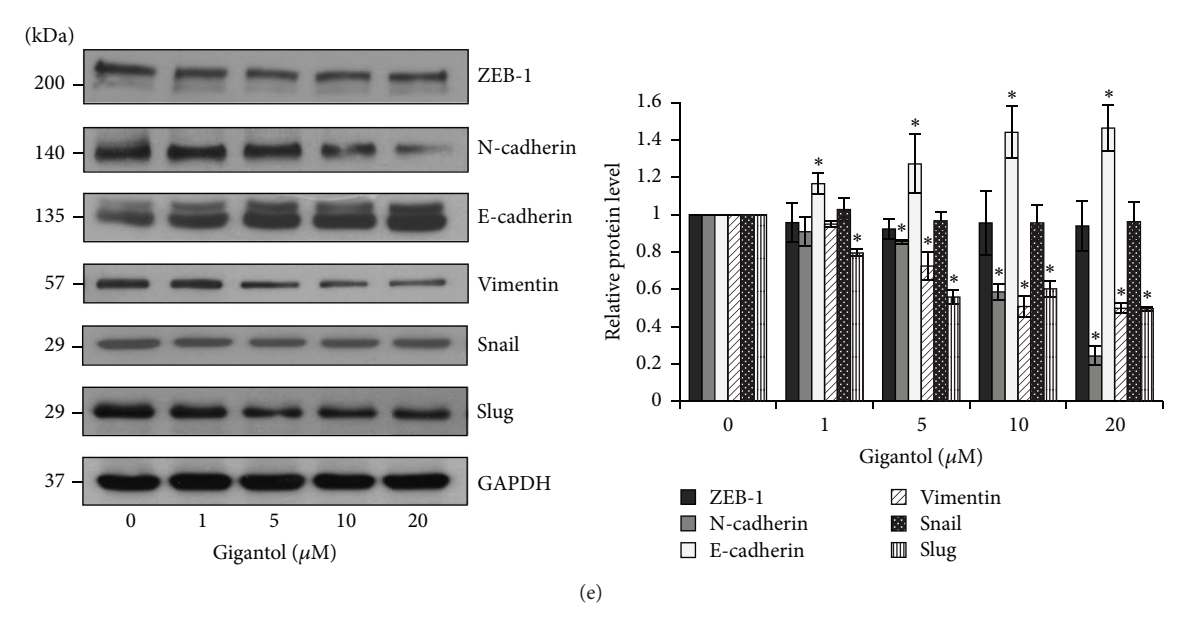


FIGURE 3: Effect of gigantol on epithelial to mesenchymal process (EMT) in human lung cancer cell H460. (a) H460 cells were treated with noncytotoxic doses of gigantol (0–20 μ M) for 24 h. Wound space was photographed and analyzed at 0, 24, 48, and 72 h. The relative migration level was calculated as the changes of wound space of the treatment groups compared to that of the untreated control group at the indicated time. (b) H460 cells migration was examined using transwell migration assay. After 24 h the migrated cells were stained with Hoechst 33342 and visualized by fluorescence microscopy (*scale bar* is 50 μ m). The relative migration level was calculated as the number of migrated cells of the treatment groups divided by that of the untreated control group. (c) H460 cells invasion was examined using transwell invasion assay. After 24 h the invaded cells were stained with Hoechst 33342 and visualized by fluorescence microscopy (*scale bar* is 50 μ m). The relative invasion level was calculated as the number of migrated cells of the treatment groups divided by that of the untreated control group. (d) The effect of gigantol on migratory-related proteins. After H460 cells were treated with noncytotoxic doses of gigantol (0–20 μ M) for 24 h, the expression of Rho GTP and Rac GTP was evaluated using Western blot assay. (e) The effect of gigantol on EMT marker proteins. After H460 cells were treated with noncytotoxic doses of gigantol (0–20 μ M) for 24 h, the expressions of N-cadherin, E-cadherin, Vimentin, Snail, Slug, and ZEB-1 were evaluated using Western blot assay. The blots were reprobed with GAPDH to confirm equal loading. The immunoblot signals were qualified by densitometry. The data represent mean \pm SE (n = 4). *p < 0.05 versus untreated control cells.

the control. In contrast, CMA treatment had no effect on Slug expression levels. This finding reveals that proteasomal degradation is involved in the stability of Slug expression. It is known that ubiquitination is a critical prerequisite and a rate-limiting step prior to proteasomal cleavage. Because of this fact, we investigated Slug-ubiquitin complexes in response to gigantol treatment using an immunoprecipitation assay. Figure 4(b) shows that the H460 cells treated with gigantol exhibited significant increases in Slug-ubiquitin complex levels, despite the equally loaded Slug expression in the control and the treatment groups. This suggests that gigantol is able to enhance Slug degradation via the proteasomal pathway.

3.4. Effect of Gigantol on EMT Regulating Proteins. To further examine the signaling pathway of gigantol in inhibiting the EMT process, the expression levels of the upstream proteins were evaluated. It has been shown that GSK-3 β is the protein responsible for Slug ubiquitination. Figure 5(a) shows that gigantol treatment decreased inactivated GSK-3 β (p-GSK-3 β) levels, indicating that GSK-3 β Slug destabilization was increased. Moreover, β -catenin is known as an essential transcriptional activator of Slug expression [10]. Interestingly, Figure 5(a) clearly shows that treatment with gigantol could decrease β -catenin expression. Moreover, previous studies

have indicated that AKT enhancement drives epithelial cells towards transdifferentiation [10]. The data shown in Figure 5(a) demonstrate that AKT phosphorylation was significantly reduced in response to gigantol treatment. These results suggest that gigantol attenuates EMT via AKT down-regulation, leading to a decrease in β -catenin expression and an increase in GSK-3 β activity.

To further confirm that the inhibition of AKT phosphorylation is able to interfere with downstream proteins, H460 cells were treated with the AKT inhibitor, perifosine. The data shown in Figure 5(b) confirm that perifosine treatment suppressed AKT phosphorylation. In addition, the β -catenin and p-GSK-3 β expression levels were significantly reduced. These results confirm that AKT activation could influence the expression of downstream proteins and the EMT process.

4. Discussion

Cancer metastasis is a fundamental cause of death in lung cancer patients. The essential driving force towards metastasis is the morphological transition of cells known as epithelial to mesenchymal transition [3]. This transition in cellular phenotype facilitates the aggressiveness of cancer by enhancing cellular migration levels and anoikis resistance. Several studies

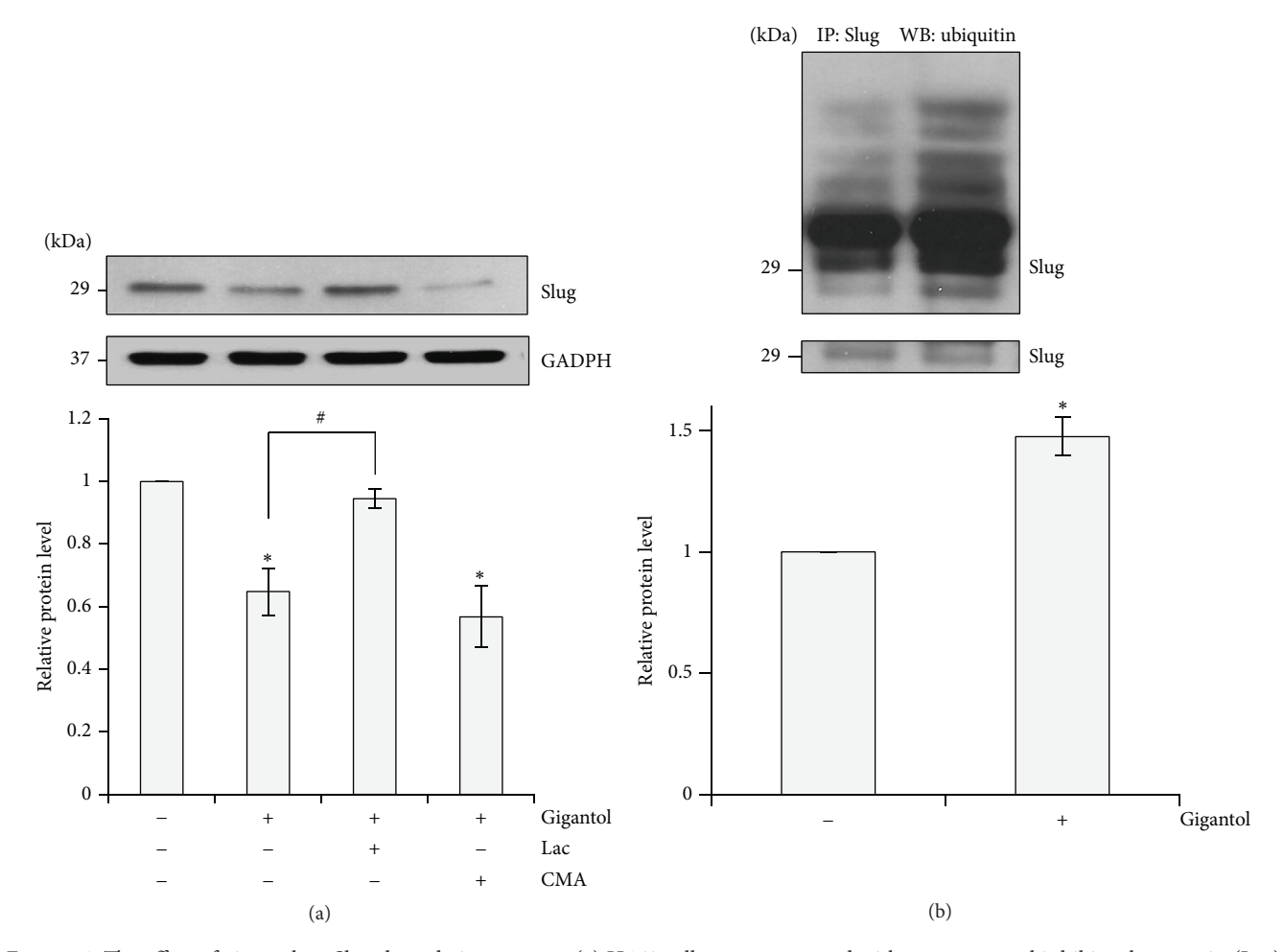


FIGURE 4: The effect of gigantol on Slug degradation process. (a) H460 cells were pretreated with a proteasomal inhibitor lactacystin (Lac) 10 μ M or lysosomal inhibitor concanamycin A (CMA) 1 μ M for an hour before treatment with 20 μ M of gigantol for 24 h. Slug expression was analyzed using Western blotting assay. The immunoblot signals were qualified by densitometry. The data represent mean \pm SE (n=4). *p<0.05 versus untreated control cells *p<0.05 versus gigantol treated cells. (b) H460 cells were pretreated with lactacystin (Lac) 10 μ M for an hour, and then the pretreated cells were exposed to a presence of gigantol or left untreated for 3 h. The levels of immunocomplexes were analyzed for ubiquitin using anti-ubiquitin antibody. The blot was reprobed with Slug antibody to confirm the equal basal amount of Slug. Immunoblot signals were qualified by densitometry. The data represent mean \pm SE (n=4). *p<0.05 versus control cells.

have identified various natural compounds with the ability to attenuate cancer metastasis. It has been reported that gigantol, a stilbenoid derivative extracted from *Dendrobium draconis*, possesses promising anticancer properties [18–20, 28]. In this study, we have provided further molecular evidence supporting the potential of gigantol as a biological agent for cancer treatment. Our results demonstrate that noncytotoxic concentrations of gigantol are able to significantly inhibit migratory behavior and decrease the level of EMT marker proteins (Figure 3). Moreover, our findings indicate that these inhibitory effects are involved in gigantol downregulation of Slug, a major transcription factor underlying EMT [12, 13].

Previous studies have reported that gigantol inhibits migration and sensitizes anoikis in lung cancer cells [18, 28]. However, scientific evidence on the underlying mechanisms of upstream pathways remained unknown. Consistent with a previous report [18], our results demonstrate that gigantol

inhibits the ability of lung cancer cells to migrate. Interestingly, in the present study, gigantol pretreatment occurred 24 h prior to the migration evaluation, and we found that the inhibition of migration persisted up to 72 h after gigantol treatment was removed (Figure 3). This finding provides novel evidence that gigantol possesses the ability to affect upstream mechanisms of migration.

It is widely accepted that cellular migration and anoikis resistance are properties of the EMT process [7, 29–31]. We therefore hypothesized that gigantol may attenuate the transdifferentiation process. Our protein expression analysis demonstrated that gigantol was able to significantly reduce the expression of EMT markers including N-cadherin and Vimentin while enhancing the expression of E-cadherin 24 h after treatment (Figure 3). Slug, the main regulator of EMT, acts as a molecular switch that suppresses E-cadherin expression by blocking a set of E-cadherin encoding genes. Our

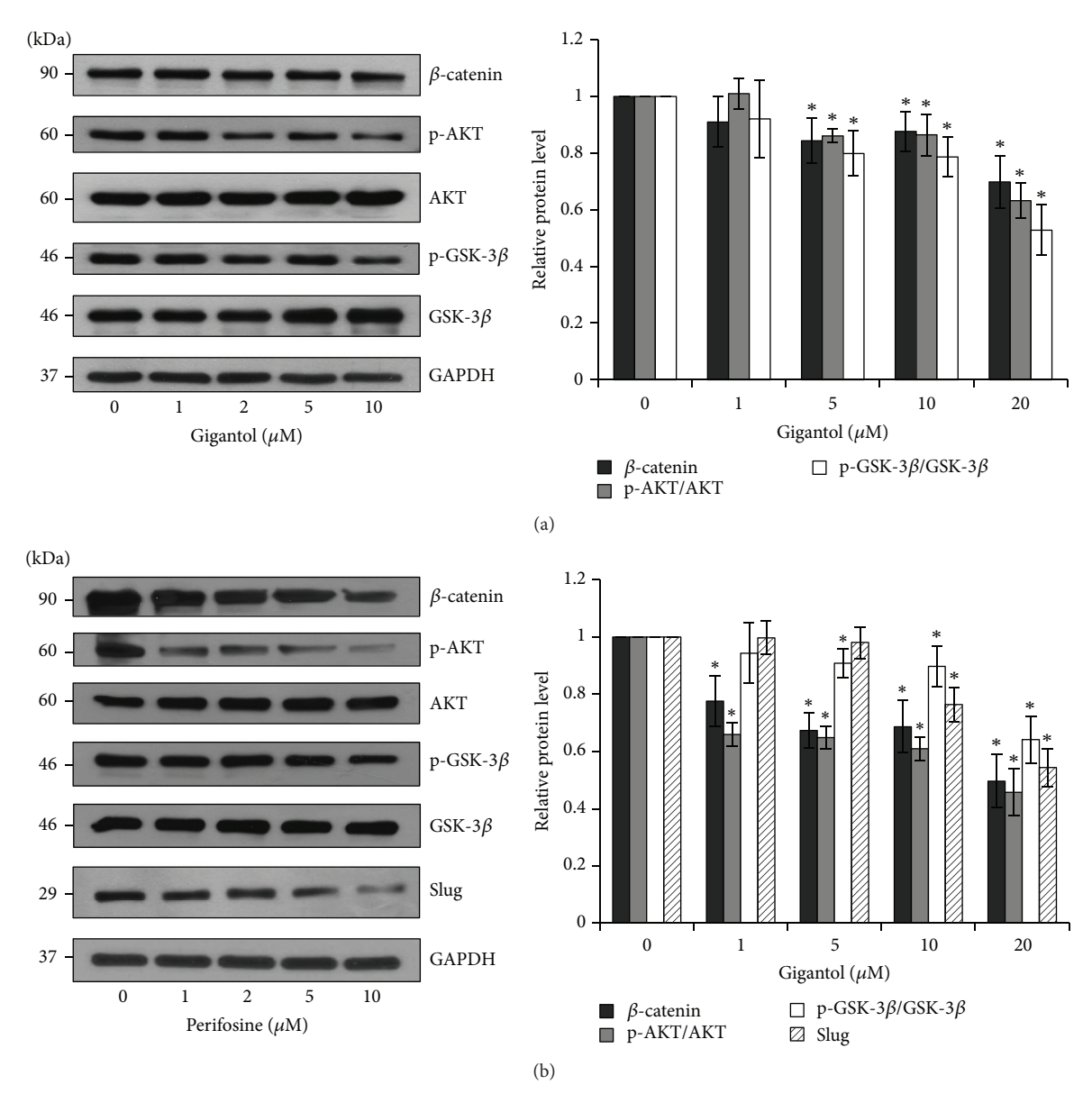


FIGURE 5: The effect of gigantol on EMT regulating proteins. (a) After H460 cells were treated with noncytotoxic doses of gigantol (0–20 μ M), the expression of β -catenin, phosphorylated AKT (Ser473), AKT, phosphorylated GSK-3 β (Ser9), and GSK-3 β was evaluated using Western blot assay. (b) AKT inhibitor, perifosine, was used to treat H460 cells (0–10 μ M); the expression of β -catenin, phosphorylated AKT (Ser473), AKT, phosphorylated GSK-3 β (Ser9), GSK-3 β , and Slug was evaluated using Western blot assay. The blots were reprobed with GAPDH to confirm equal loading. The immunoblot signals were qualified by densitometry. The data represent mean \pm SE (n=4). *p<0.05 versus untreated control cells.

results show that gigantol treatment significantly suppressed the expression of the Slug transcription factor. It was also observed that gigantol did not affect Snail or ZEB-1 expression. It appears that Slug is the main target of gigantol treatment. Another possibility is that Snail was claimed to be an unstable protein. So the effect of gigantol on the expression of Slug may be detectable but not Snail or ZEB-1. This finding suggests that gigantol was able to attenuate the EMT process at the transcriptional level. β -catenin and GSK-3 β proteins may regulate the expression of the Slug transcription factor via production and degradation pathways, respectively [12].

In epithelial cells, β -catenin interacts with the cytoplasmic domain of E-cadherin, whereas, during the EMT process, β -catenin is released from the complex and translocated into the nucleus to increase the expression of Slug. On the other hand, activated GSK-3 β causes Slug phosphorylation in the central domain, leading to Slug ubiquitination and, consequently, proteasomal degradation [12]. GSK-3 β can be inactivated through phosphorylation. The results illustrated in Figure 5(a) indicate that gigantol treatment not only decreased Slug expression by promoting the degradation pathway but also suppressed its transcriptional activation.

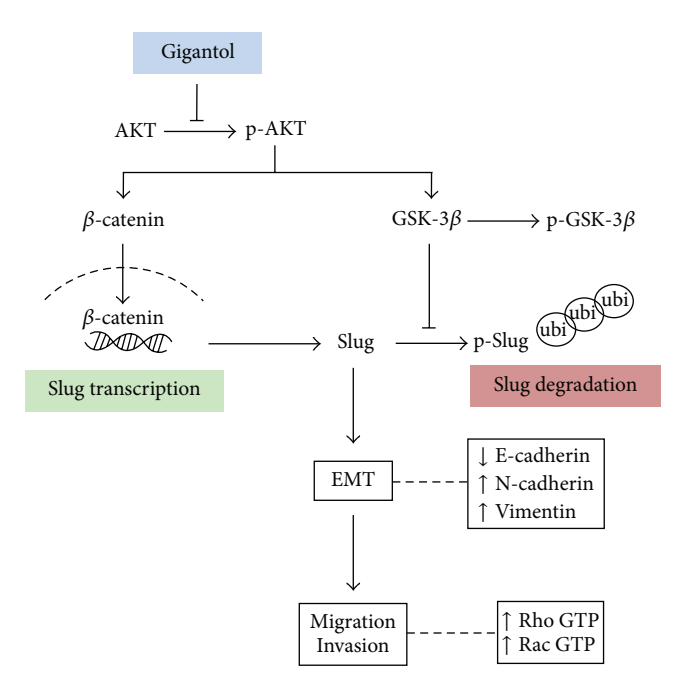


FIGURE 6: A schematic diagram summarizes the EMT inhibitory mechanism of gigantol on lung cancer cells. Gigantol suppresses the activation of AKT resulting in a decrease in Slug by both decreasing the production and increasing the degradation processes.

Many studies have demonstrated that activated AKT plays an important role in the EMT process [10, 32]. As evidenced by a previous report, gigantol inhibited migration by decreasing the function of AKT [18]. However, in the present study, it was shown that AKT activation was significantly suppressed within the first 3 h of gigantol treatment (Figure 5(a)). Therefore, it is possible that gigantol may affect the upstream signaling pathway to attenuate migration behavior. These data are consistent with previous studies that show that the attenuation of AKT activity was able to suppress the expression of Slug and inhibit mesenchymal transition through the β catenin and GSK-3 β pathways [32–34]. It has been demonstrated that the activation of AKT positively regulates Slug transcription via β -catenin in vitro [35] and suppresses Slug degradation [36]. The inhibition of AKT could be a promising therapeutic approach to attenuate the EMT process.

5. Conclusion

In conclusion, this study has demonstrated that gigantol is able to attenuate the EMT process in lung cancer cells. The reduction of AKT activity decreased the transcription and the stability of Slug. Gigantol was shown to reduce β -catenin activity and Slug transcription while enhancing GSK-3 β ubiquitination of Slug, resulting in decreased Slug levels and thereby suppressing the EMT process (Figure 6). This novel discovery supports the future development of gigantol as an antimetastasis treatment in cancer patients.

Competing Interests

The authors declare that they have no competing interests.

Acknowledgments

The research was supported by Thailand Research Fund (MRG 5980021).

References

- [1] D. Kong, Y. Li, Z. Wang, and F. H. Sarkar, "Cancer stem cells and Epithelial-to-Mesenchymal Transition (EMT)-phenotypic cells: are they cousins or twins?" *Cancers*, vol. 3, no. 1, pp. 716–729, 2011.
- [2] X. Chen, J. Zhang, Z. Zhang, H. Li, W. Cheng, and J. Liu, "Cancer stem cells, epithelial-mesenchymal transition, and drug resistance in high-grade ovarian serous carcinoma," *Human Pathology*, vol. 44, no. 11, pp. 2373–2384, 2013.
- [3] T. R. Geiger and D. S. Peeper, "Metastasis mechanisms," Biochimica et Biophysica Acta (BBA)—Reviews on Cancer, vol. 1796, no. 2, pp. 293–308, 2009.
- [4] American Cancer Society, Cancer Facts & Figures, American Cancer Society, Atlanta, Ga, USA, 2016.
- [5] J. Pasquier, N. Abu-Kaoud, A. I. Thani, and A. Rafii, "Epithelial to mesenchymal transition in a clinical perspective," *Journal of Oncology*, vol. 2015, Article ID 792182, 10 pages, 2015.
- [6] M. Iwatsuki, K. Mimori, T. Yokobori et al., "Epithelial-mesenchymal transition in cancer development and its clinical significance," *Cancer Science*, vol. 101, no. 2, pp. 293–299, 2010.
- [7] A. Voulgari and A. Pintzas, "Epithelial-mesenchymal transition in cancer metastasis: mechanisms, markers and strategies to overcome drug resistance in the clinic," *Biochimica et Biophysica Acta*, vol. 1796, no. 2, pp. 75–90, 2009.
- [8] S. Kumar, S. H. Park, B. Cieply et al., "A pathway for the control of anoikis sensitivity by E-cadherin and epithelial-tomesenchymal transition," *Molecular and Cellular Biology*, vol. 31, no. 19, pp. 4036–4051, 2011.
- [9] Y. Shi, H. Wu, M. Zhang, L. Ding, F. Meng, and X. Fan, "Expression of the epithelial-mesenchymal transition-related proteins and their clinical significance in lung adenocarcinoma," *Diagnostic Pathology*, vol. 8, no. 1, article 89, pp. 1–8, 2013.
- [10] S. Lamouille, J. Xu, and R. Derynck, "Molecular mechanisms of epithelial-mesenchymal transition," *Nature Reviews Molecular Cell Biology*, vol. 15, no. 3, pp. 178–196, 2014.
- [11] M. J. Wheelock, Y. Shintani, M. Maeda, Y. Fukumoto, and K. R. Johnson, "Cadherin switching," *Journal of Cell Science*, vol. 121, no. 6, pp. 727–735, 2008.
- [12] K. Lee and C. M. Nelson, "Insights into the regulation of epithelial-mesenchymal transition and tissue fibrosis," *The Journal of Cell Biology*, vol. 294, pp. 171–221, 2012.
- [13] A. Barrallo-Gimeno and M. A. Nieto, "The Snail genes as inducers of cell movement and survival: implications in development and cancer," *Development*, vol. 132, no. 14, pp. 3151–3161, 2005.
- [14] S. M. Frisch, M. Schaller, and B. Cieply, "Mechanisms that link the oncogenic epithelial-mesenchymal transition to suppression of anoikis," *Journal of Cell Science*, vol. 126, no. 1, pp. 21–29, 2013.

- [15] E. Sánchez-Tilló, Y. Liu, O. De Barrios et al., "EMT-activating transcription factors in cancer: beyond EMT and tumor invasiveness," *Cellular and Molecular Life Sciences*, vol. 69, no. 20, pp. 3429–3456, 2012.
- [16] Y. Wang, J. Shi, K. Chai, X. Ying, and B. P. Zhou, "The role of Snail in EMT and tumorigenesis," *Current Cancer Drug Targets*, vol. 13, no. 9, pp. 963–972, 2013.
- [17] J.-Y. Shih and P.-C. Yang, "The EMT regulator slug and lung carcinogenesis," *Carcinogenesis*, vol. 32, no. 9, pp. 1299–1304, 2011.
- [18] S. Charoenrungruang, P. Chanvorachote, B. Sritularak, and V. Pongrakhananon, "Gigantol, a bibenzyl from *Dendrobium draconis*, inhibits the migratory behavior of non-small cell lung cancer cells," *Journal of Natural Products*, vol. 77, no. 6, pp. 1359–1366, 2014.
- [19] S. Charoenrungruang, P. Chanvorachote, and B. Sritularak, "Gigantol-induced apoptosis in lung cancer cell through mitochondrial-dependent pathway," *Thai Journal of Pharma-ceutical Sciences*, vol. 38, no. 2, pp. 67–73, 2014.
- [20] N. Bhummaphan and P. Chanvorachote, "Gigantol suppresses cancer stem cell-like phenotypes in lung cancer cells," Evidence-Based Complementary and Alternative Medicine, vol. 2015, Article ID 836564, 10 pages, 2015.
- [21] C.-K. Ho and C.-C. Chen, "Moscatilin from the orchid *Dendrobrium loddigesii* is a potential anticancer agent," *Cancer Investigation*, vol. 21, no. 5, pp. 729–736, 2003.
- [22] P. Klongkumnuankarn, K. Busaranon, P. Chanvorachote, B. Sritularak, V. Jongbunprasert, and K. Likhitwitayawuid, "Cytotoxic and antimigratory activities of phenolic compounds from Dendrobium brymerianum," Evidence-Based Complementary and Alternative Medicine, vol. 2015, Article ID 350410, 9 pages, 2015.
- [23] B. Sritularak, M. Anuwat, and K. Likhitwitayawuid, "A new phenanthrenequinone from *Dendrobium draconis*," *Journal of Asian Natural Products Research*, vol. 13, no. 3, pp. 251–255, 2011.
- [24] L. S. Price, J. Leng, M. A. Schwartz, and G. M. Bokoch, "Activation of Rac and Cdc42 by integrins mediates cell spreading," *Molecular Biology of the Cell*, vol. 9, no. 7, pp. 1863–1871, 1998.
- [25] L. Van Aelst and M. Symons, "Role of Rho family GTPases in epithelial morphogenesis," *Genes & Development*, vol. 16, no. 9, pp. 1032–1054, 2002.
- [26] X. Zhao and J.-L. Guan, "Focal adhesion kinase and its signaling pathways in cell migration and angiogenesis," Advanced Drug Delivery Reviews, vol. 63, no. 8, pp. 610–615, 2011.
- [27] Y. Wu, B. M. Evers, and B. P. Zhou, "Small C-terminal domain phosphatase enhances snail activity through dephosphorylation," *The Journal of Biological Chemistry*, vol. 284, no. 1, pp. 640–648, 2009.
- [28] T. Unahabhokha, P. Chanvorachote, and V. Pongrakhananon, "The attenuation of epithelial to mesenchymal transition and induction of anoikis by gigantol in human lung cancer H460 cells," *Tumor Biology*, 2016.
- [29] P. Chiarugi and E. Giannoni, "Anoikis: a necessary death program for anchorage-dependent cells," *Biochemical Pharma-cology*, vol. 76, no. 11, pp. 1352–1364, 2008.
- [30] F. Nurwidya, F. Takahashi, A. Murakami, and K. Takahashi, "Epithelial mesenchymal transition in drug resistance and metastasis of lung cancer," *Cancer Research and Treatment*, vol. 44, no. 3, pp. 151–156, 2012.
- [31] N. Fenouille, M. Tichet, M. Dufies et al., "The epithelial-mesenchymal transition (EMT) regulatory factor SLUG

- (SNAI2) is a downstream target of SPARC and AKT in promoting melanoma cell invasion," *PLoS ONE*, vol. 7, no. 7, Article ID e40378, pp. 1–15, 2012.
- [32] C. Kiratipaiboon, P. Tengamnuay, and P. Chanvorachote, "Ciprofloxacin improves the stemness of human dermal papilla cells," *Stem Cells International*, vol. 2016, Article ID 5831276, 14 pages, 2016.
- [33] S. Zhao, J. Fu, X. Liu, T. Wang, J. Zhang, and Y. Zhao, "Activation of Akt/GSK-3beta/beta-catenin signaling pathway is involved in survival of neurons after traumatic brain injury in rats," *Neurological Research*, vol. 34, no. 4, pp. 400–407, 2012.
- [34] D. Fang, D. Hawke, Y. Zheng et al., "Phosphorylation of β -catenin by AKT promotes β -catenin transcriptional activity," *The Journal of Biological Chemistry*, vol. 282, no. 15, pp. 11221–11229, 2007.
- [35] T.-S. Huang, L. Li, L. Moalim-Nour et al., "A regulatory network involving β -catenin, e-cadherin, PI3k/Akt, and slug balances self-renewal and differentiation of human pluripotent stem cells in response to wnt signaling," *STEM CELLS*, vol. 33, no. 5, pp. 1419–1433, 2015.
- [36] S.-H. Kao, W.-L. Wang, C.-Y. Chen et al., "GSK3 β controls epithelial-mesenchymal transition and tumor metastasis by CHIP-mediated degradation of slug," *Oncogene*, vol. 33, no. 24, pp. 3172–3182, 2014.